

18

Molecular interactions

Electric properties of molecules

18.1 Electric dipole moments

18.2 Polarizabilities

18.3 Relative permittivities

Interactions between molecules

18.4 Interactions between dipoles

18.5 Repulsive and total interactions

I18.1 Impact on medicine:
Molecular recognition and
drug design

Gases and liquids

18.6 Molecular interactions in gases

18.7 The liquid–vapour interface

18.8 Condensation

Checklist of key ideas

Further reading

Further information 18.1: The
dipole–dipole interaction

Further information 18.2: The basic
principles of molecular beams

Discussion questions

Exercises

Problems

In this chapter we examine molecular interactions in gases and liquids and interpret them in terms of electric properties of molecules, such as electric dipole moments and polarizabilities. All these properties reflect the degree to which the nuclei of atoms exert control over the electrons in a molecule, either by causing electrons to accumulate in particular regions, or by permitting them to respond more or less strongly to the effects of external electric fields.

Molecular interactions are responsible for the unique properties of substances as simple as water and as complex as polymers. We begin our examination of molecular interactions by describing the electric properties of molecules, which may be interpreted in terms of concepts in electronic structure introduced in Chapter 11. We shall see that small imbalances of charge distributions in molecules allow them to interact with one another and with externally applied fields. One result of this interaction is the cohesion of molecules to form the bulk phases of matter. These interactions are also important for understanding the shapes adopted by biological and synthetic macromolecules, as we shall see in Chapter 19. The interaction between ions is treated in Chapter 5 (for solutions) and Chapter 20 (for solids).

Electric properties of molecules

Many of the electric properties of molecules can be traced to the competing influences of nuclei with different charges or the competition between the control exercised by a nucleus and the influence of an externally applied field. The former competition may result in an electric dipole moment. The latter may result in properties such as refractive index and optical activity.

18.1 Electric dipole moments

An **electric dipole** consists of two electric charges $+q$ and $-q$ separated by a distance R . This arrangement of charges is represented by a vector μ (1). The magnitude of μ is $\mu = qR$ and, although the SI unit of dipole moment is coulomb metre ($C\ m$), it is still commonly reported in the non-SI unit debye, D, named after Peter Debye, a pioneer in the study of dipole moments of molecules, where

$$1\ D = 3.335\ 64 \times 10^{-30}\ C\ m \quad (18.1)$$

The dipole moment of a pair of charges $+e$ and $-e$ separated by 100 pm is $1.6 \times 10^{-29}\ C\ m$, corresponding to 4.8 D. Dipole moments of small molecules are typically about 1 D. The conversion factor in eqn 18.1 stems from the original definition of the debye in terms of c.g.s. units: 1 D is the dipole moment of two equal and opposite charges of magnitude 1 e.s.u. separated by 1 Å.

(a) Polar molecules

A **polar molecule** is a molecule with a permanent electric dipole moment. The permanent dipole moment stems from the partial charges on the atoms in the molecule that arise from differences in electronegativity or other features of bonding (Section 11.6). Nonpolar molecules acquire an induced dipole moment in an electric field on account of the distortion the field causes in their electronic distributions and nuclear positions; however, this induced moment is only temporary, and disappears as soon as the perturbing field is removed. Polar molecules also have their existing dipole moments temporarily modified by an applied field.

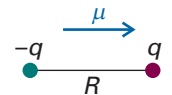
The Stark effect (Section 13.5) is used to measure the electric dipole moments of molecules for which a rotational spectrum can be observed. In many cases microwave spectroscopy cannot be used because the sample is not volatile, decomposes on vaporization, or consists of molecules that are so complex that their rotational spectra cannot be interpreted. In such cases the dipole moment may be obtained by measurements on a liquid or solid bulk sample using a method explained later. Computational software is now widely available, and typically computes electric dipole moments by assessing the electron density at each point in the molecule and its coordinates relative to the centroid of the molecule; however, it is still important to be able to formulate simple models of the origin of these moments and to understand how they arise. The following paragraphs focus on this aspect.

All heteronuclear diatomic molecules are polar, and typical values of μ include 1.08 D for HCl and 0.42 D for HI (Table 18.1). Molecular symmetry is of the greatest importance in deciding whether a polyatomic molecule is polar or not. Indeed, molecular symmetry is more important than the question of whether or not the atoms in the molecule belong to the same element. Homonuclear polyatomic molecules may be polar if they have low symmetry and the atoms are in inequivalent positions. For instance, the angular molecule ozone, O_3 (2), is homonuclear; however, it is polar because the central O atom is different from the outer two (it is bonded to two atoms, they are bonded only to one); moreover, the dipole moments associated with each bond make an angle to each other and do not cancel. Heteronuclear polyatomic molecules may be nonpolar if they have high symmetry, because individual bond dipoles may then cancel. The heteronuclear linear triatomic molecule CO_2 , for example, is nonpolar because, although there are partial charges on all three atoms, the dipole moment associated with the OC bond points in the opposite direction to the dipole moment associated with the CO bond, and the two cancel (3).

To a first approximation, it is possible to resolve the dipole moment of a polyatomic molecule into contributions from various groups of atoms in the molecule and the directions in which these individual contributions lie (Fig. 18.1). Thus,

| Synoptic table 18.1* | | |
|----------------------|---------|----------------------------------|
| | μ/D | $\alpha'/(10^{-30} \text{ m}^3)$ |
| CCl_4 | 0 | 10.5 |
| H_2 | 0 | 0.819 |
| H_2O | 1.85 | 1.48 |
| HCl | 1.08 | 2.63 |
| HI | 0.42 | 5.45 |

* More values are given in the *Data section*.



1 Electric dipole

Comment 18.1

In elementary chemistry, an electric dipole moment is represented by the arrow \rightarrow added to the Lewis structure for the molecule, with the $+$ marking the positive end. Note that the direction of the arrow is opposite to that of μ .

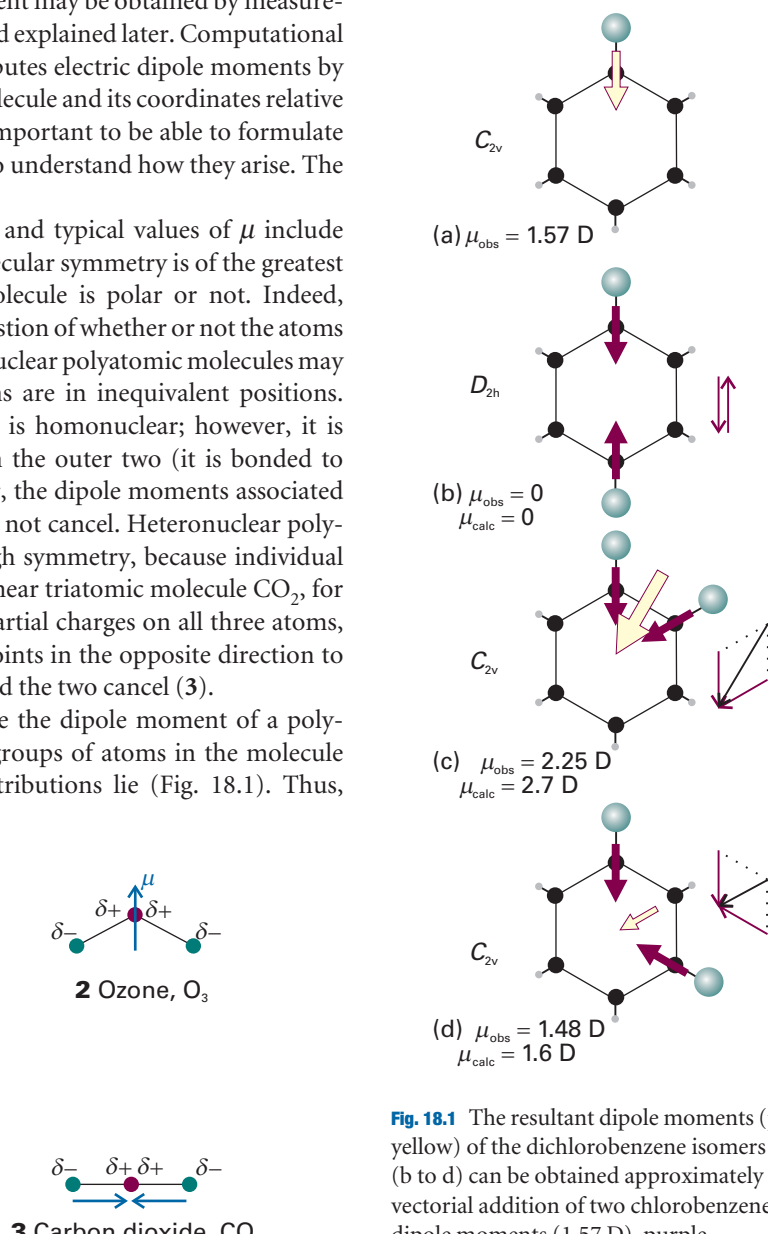
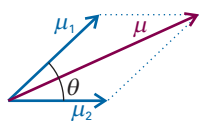


Fig. 18.1 The resultant dipole moments (pale yellow) of the dichlorobenzene isomers (b to d) can be obtained approximately by vectorial addition of two chlorobenzene dipole moments (1.57 D), purple.



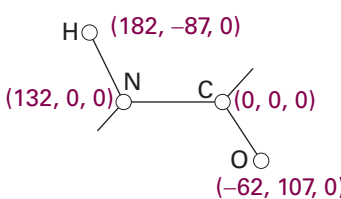
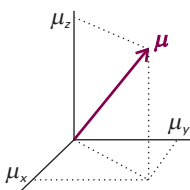
4 Addition of dipole moments

Comment 18.2

Operations involving vectors are described in Appendix 2, where eqn 18.2 is also derived.

Comment 18.3

In three dimensions, a vector μ has components μ_x , μ_y , and μ_z along the x -, y -, and z -axes, respectively, as shown in the illustration. The direction of each of the components is denoted with a plus sign or minus sign. For example, if $\mu_x = -1.0$ D, the x -component of the vector μ has a magnitude of 1.0 D and points in the $-x$ direction.



5 Amide group

Table 18.2 Partial charges in polypeptides

| Atom | Partial charge/e |
|--------|------------------|
| C(=O) | +0.45 |
| C(-CO) | +0.06 |
| H(-C) | +0.02 |
| H(-N) | +0.18 |
| H(-O) | +0.42 |
| N | -0.36 |
| O | -0.38 |

1,4-dichlorobenzene is nonpolar by symmetry on account of the cancellation of two equal but opposing C—Cl moments (exactly as in carbon dioxide). 1,2-Dichlorobenzene, however, has a dipole moment which is approximately the resultant of two chlorobenzene dipole moments arranged at 60° to each other. This technique of ‘vector addition’ can be applied with fair success to other series of related molecules, and the resultant μ_{res} of two dipole moments μ_1 and μ_2 that make an angle θ to each other (4) is approximately

$$\mu_{\text{res}} \approx (\mu_1^2 + \mu_2^2 + 2\mu_1\mu_2 \cos \theta)^{1/2} \quad (18.2a)$$

When the two dipole moments have the same magnitude (as in the dichlorobenzenes), this equation simplifies to

$$\mu_{\text{res}} \approx 2\mu_1 \cos \frac{1}{2}\theta \quad (18.2b)$$

Self-test 18.1 Estimate the ratio of the electric dipole moments of *ortho* (1,2-) and *meta* (1,3-) disubstituted benzenes. $[\mu(\text{ortho})/\mu(\text{meta}) = 1.7]$

A better approach to the calculation of dipole moments is to take into account the locations and magnitudes of the partial charges on all the atoms. These partial charges are included in the output of many molecular structure software packages. To calculate the x -component, for instance, we need to know the partial charge on each atom and the atom’s x -coordinate relative to a point in the molecule and form the sum

$$\mu_x = \sum_j q_j x_j \quad (18.3a)$$

Here q_j is the partial charge of atom J, x_j is the x -coordinate of atom J, and the sum is over all the atoms in the molecule. Analogous expressions are used for the y - and z -components. For an electrically neutral molecule, the origin of the coordinates is arbitrary, so it is best chosen to simplify the measurements. In common with all vectors, the magnitude of μ is related to the three components μ_x , μ_y , and μ_z by

$$\mu = (\mu_x^2 + \mu_y^2 + \mu_z^2)^{1/2} \quad (18.3b)$$

Example 18.1 Calculating a molecular dipole moment

Estimate the electric dipole moment of the amide group shown in (5) by using the partial charges (as multiples of e) in Table 18.2 and the locations of the atoms shown.

Method We use eqn 18.3a to calculate each of the components of the dipole moment and then eqn 18.3b to assemble the three components into the magnitude of the dipole moment. Note that the partial charges are multiples of the fundamental charge, $e = 1.609 \times 10^{-19}$ C.

Answer The expression for μ_x is

$$\begin{aligned} \mu_x &= (-0.36e) \times (132 \text{ pm}) + (0.45e) \times (0 \text{ pm}) + (0.18e) \times (182 \text{ pm}) \\ &\quad + (-0.38e) \times (-62.0 \text{ pm}) \\ &= 8.8e \text{ pm} \\ &= 8.8 \times (1.609 \times 10^{-19} \text{ C}) \times (10^{-12} \text{ m}) = 1.4 \times 10^{-30} \text{ C m} \end{aligned}$$

corresponding to $\mu_x = 0.42$ D. The expression for μ_y is:

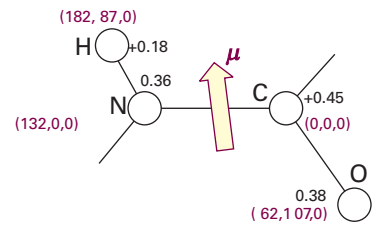
$$\begin{aligned}\mu_y &= (-0.36e) \times (0 \text{ pm}) + (0.45e) \times (0 \text{ pm}) + (0.18e) \times (-86.6 \text{ pm}) \\ &\quad + (-0.38e) \times (107 \text{ pm}) \\ &= -56e \text{ pm} = -9.1 \times 10^{-30} \text{ C m}\end{aligned}$$

It follows that $\mu_y = -2.7$ D. Therefore, because $\mu_z = 0$,

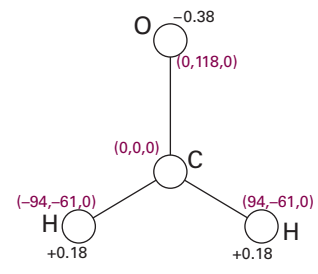
$$\mu = \{(0.42 \text{ D})^2 + (-2.7 \text{ D})^2\}^{1/2} = 2.7 \text{ D}$$

We can find the orientation of the dipole moment by arranging an arrow of length 2.7 units of length to have x , y , and z components of 0.42, -2.7, and 0 units; the orientation is superimposed on (6).

Self-test 18.2 Calculate the electric dipole moment of formaldehyde, using the information in (7). [−3.2 D]



6



7

(b) Polarization

The **polarization**, P , of a sample is the electric dipole moment density, the mean electric dipole moment of the molecules, $\langle \mu \rangle$, multiplied by the number density, \mathcal{N} :

$$P = \langle \mu \rangle \mathcal{N} \quad (18.4)$$

In the following pages we refer to the sample as a **dielectric**, by which is meant a polarizable, nonconducting medium.

The polarization of an isotropic fluid sample is zero in the absence of an applied field because the molecules adopt random orientations, so $\langle \mu \rangle = 0$. In the presence of a field, the dipoles become partially aligned because some orientations have lower energies than others. As a result, the electric dipole moment density is nonzero. We show in the *Justification* below that, at a temperature T

$$\langle \mu_z \rangle = \frac{\mu^2 E}{3kT} \quad (18.5)$$

where z is the direction of the applied field E . Moreover, as we shall see, there is an additional contribution from the dipole moment induced by the field.

Justification 18.1 The thermally averaged dipole moment

The probability dp that a dipole has an orientation in the range θ to $\theta + d\theta$ is given by the Boltzmann distribution (Section 16.1b), which in this case is

$$dp = \frac{e^{-E(\theta)/kT} \sin \theta d\theta}{\int_0^\pi e^{-E(\theta)/kT} \sin \theta d\theta}$$

where $E(\theta)$ is the energy of the dipole in the field: $E(\theta) = -\mu E \cos \theta$, with $0 \leq \theta \leq \pi$. The average value of the component of the dipole moment parallel to the applied electric field is therefore

$$\langle \mu_z \rangle = \int \mu \cos \theta dp = \mu \int \cos \theta dp = \frac{\mu \int_0^\pi e^{\mu \cos \theta} \cos \theta \sin \theta d\theta}{\int_0^\pi e^{\mu \cos \theta} \sin \theta d\theta}$$

with $x = \mu\mathcal{E}/kT$. The integral takes on a simpler appearance when we write $y = \cos \theta$ and note that $dy = -\sin \theta d\theta$.

$$\langle \mu_z \rangle = \frac{\mu \int_{-1}^1 y e^{xy} dy}{\int_{-1}^1 e^{xy} dy}$$

At this point we use

$$\int_{-1}^1 e^{xy} dy = \frac{e^x - e^{-x}}{x} \quad \int_{-1}^1 y e^{xy} dy = \frac{e^x + e^{-x}}{x} - \frac{e^x - e^{-x}}{x^2}$$

It is now straightforward algebra to combine these two results and to obtain

$$\langle \mu_z \rangle = \mu L(x) \quad L(x) = \frac{e^x + e^{-x}}{e^x - e^{-x}} - \frac{1}{x} \quad x = \frac{\mu\mathcal{E}}{kT} \quad (18.6)$$

$L(x)$ is called the **Langevin function**.

Under most circumstances, x is very small (for example, if $\mu = 1$ D and $T = 300$ K, then x exceeds 0.01 only if the field strength exceeds 100 kV cm $^{-1}$, and most measurements are done at much lower strengths). When $x \ll 1$, the exponentials in the Langevin function can be expanded, and the largest term that survives is

$$L(x) = \frac{1}{3}x + \dots \quad (18.7)$$

Therefore, the average molecular dipole moment is given by eqn 18.6.

18.2 Polarizabilities

An applied electric field can distort a molecule as well as align its permanent electric dipole moment. The **induced dipole moment**, μ^* , is generally proportional to the field strength, \mathcal{E} , and we write

$$\mu^* = \alpha \mathcal{E} \quad (18.8)$$

(See Section 20.10 for exceptions to eqn 18.8.) The constant of proportionality α is the **polarizability** of the molecule. The greater the polarizability, the larger is the induced dipole moment for a given applied field. In a formal treatment, we should use vector quantities and allow for the possibility that the induced dipole moment might not lie parallel to the applied field, but for simplicity we discuss polarizabilities in terms of (scalar) magnitudes.

(a) Polarizability volumes

Polarizability has the units (coulomb metre) 2 per joule (C 2 m 2 J $^{-1}$). That collection of units is awkward, so α is often expressed as a **polarizability volume**, α' , by using the relation

$$\alpha' = \frac{\alpha}{4\pi\epsilon_0} \quad [18.9]$$

where ϵ_0 is the vacuum permittivity. Because the units of $4\pi\epsilon_0$ are coulomb-squared per joule per metre (C 2 J $^{-1}$ m $^{-1}$), it follows that α' has the dimensions of volume (hence its name). Polarizability volumes are similar in magnitude to actual molecular volumes (of the order of 10 $^{-30}$ m 3 , 10 $^{-3}$ nm 3 , 1 Å 3).

Comment 18.4

When x is small, it is possible to simplify expressions by using the expansion $e^x = 1 + x + \frac{1}{2}x^2 + \frac{1}{6}x^3 + \dots$; it is important when developing approximations that all terms of the same order are retained because low-order terms might cancel.

Comment 18.5

When using older compilations of data, it is useful to note that polarizability volumes have the same numerical values as the ‘polarizabilities’ reported using c.g.s. electrical units, so the tabulated values previously called ‘polarizabilities’ can be used directly.

Some experimental polarizability volumes of molecules are given in Table 18.1. As shown in the *Justification* below, polarizability volumes correlate with the HOMO–LUMO separations in atoms and molecules. The electron distribution can be distorted readily if the LUMO lies close to the HOMO in energy, so the polarizability is then large. If the LUMO lies high above the HOMO, an applied field cannot perturb the electron distribution significantly, and the polarizability is low. Molecules with small HOMO–LUMO gaps are typically large, with numerous electrons.

Justification 18.2 Polarizabilities and molecular structures

When an electric field is increased by $d\mathcal{E}$, the energy of a molecule changes by $-\mu d\mathcal{E}$, and if the molecule is polarizable, we interpret μ as μ^* (eqn 18.8). Therefore, the change in energy when the field is increased from 0 to \mathcal{E} is

$$\Delta E = - \int_0^{\mathcal{E}} \mu^* d\mathcal{E} = - \int_0^{\mathcal{E}} \alpha \mathcal{E} d\mathcal{E} = -\frac{1}{2} \alpha \mathcal{E}^2$$

The contribution to the hamiltonian when a dipole moment is exposed to an electric field \mathcal{E} in the z -direction is

$$H^{(1)} = -\mu_z \mathcal{E}$$

Comparison of these two expressions suggests that we should use second-order perturbation theory to calculate the energy of the system in the presence of the field, because then we shall obtain an expression proportional to \mathcal{E}^2 . According to eqn 9.65b, the second-order contribution to the energy is

$$E^{(2)} = \sum_n \left| \frac{\int \psi_n^* H^{(1)} \psi_0 d\tau}{E_0^{(0)} - E_n^{(0)}} \right|^2 = \mathcal{E}^2 \sum_n \left| \frac{\int \psi_n^* \mu_z \psi_0 d\tau}{E_0^{(0)} - E_n^{(0)}} \right|^2 = \mathcal{E}^2 \sum_n \frac{|\mu_{z,0n}|^2}{E_0^{(0)} - E_n^{(0)}}$$

where $\mu_{z,0n}$ is the *transition* electric dipole moment in the z -direction (eqn 9.70). By comparing the two expressions for the energy, we conclude that the polarizability of the molecule in the z -direction is

$$\alpha = 2 \sum_n \frac{|\mu_{z,0n}|^2}{E_n^{(0)} - E_0^{(0)}} \quad (18.10)$$

The content of eqn 18.10 can be appreciated by approximating the excitation energies by a mean value ΔE (an indication of the HOMO–LUMO separation), and supposing that the most important transition dipole moment is approximately equal to the charge of an electron multiplied by the radius, R , of the molecule. Then

$$\alpha \approx \frac{2e^2 R^2}{\Delta E}$$

This expression shows that α increases with the size of the molecule and with the ease with which it can be excited (the smaller the value of ΔE).

If the excitation energy is approximated by the energy needed to remove an electron to infinity from a distance R from a single positive charge, we can write $\Delta E \approx e^2/4\pi\epsilon_0 R$. When this expression is substituted into the equation above, both sides are divided by $4\pi\epsilon_0$, and the factor of 2 ignored in this approximation, we obtain $\alpha' \approx R^3$, which is of the same order of magnitude as the molecular volume.

For most molecules, the polarizability is anisotropic, by which is meant that its value depends on the orientation of the molecule relative to the field. The polarizability volume of benzene when the field is applied perpendicular to the ring is 0.0067 nm^3

and it is 0.0123 nm^3 when the field is applied in the plane of the ring. The anisotropy of the polarizability determines whether a molecule is rotationally Raman active (Section 13.7).

(b) Polarization at high frequencies

When the applied field changes direction slowly, the permanent dipole moment has time to reorientate—the whole molecule rotates into a new direction—and follow the field. However, when the frequency of the field is high, a molecule cannot change direction fast enough to follow the change in direction of the applied field and the dipole moment then makes no contribution to the polarization of the sample. Because a molecule takes about 1 ps to turn through about 1 radian in a fluid, the loss of this contribution to the polarization occurs when measurements are made at frequencies greater than about 10^{11} Hz (in the microwave region). We say that the **orientation polarization**, the polarization arising from the permanent dipole moments, is lost at such high frequencies.

The next contribution to the polarization to be lost as the frequency is raised is the **distortion polarization**, the polarization that arises from the distortion of the positions of the nuclei by the applied field. The molecule is bent and stretched by the applied field, and the molecular dipole moment changes accordingly. The time taken for a molecule to bend is approximately the inverse of the molecular vibrational frequency, so the distortion polarization disappears when the frequency of the radiation is increased through the infrared. The disappearance of polarization occurs in stages: as shown in the *Justification* below, each successive stage occurs as the incident frequency rises above the frequency of a particular mode of vibration.

At even higher frequencies, in the visible region, only the electrons are mobile enough to respond to the rapidly changing direction of the applied field. The polarization that remains is now due entirely to the distortion of the electron distribution, and the surviving contribution to the molecular polarizability is called the **electronic polarizability**.

Justification 18.3 The frequency-dependence of polarizabilities

The quantum mechanical expression for the polarizability of a molecule in the presence of an electric field that is oscillating at a frequency ω in the z -direction is obtained by using time-dependent perturbation theory (*Further information 9.2*) and is

$$\alpha(\omega) = \frac{2}{\hbar} \sum_n \frac{\omega_{n0} |\mu_{z,0n}|^2}{\omega_{n0}^2 - \omega^2} \quad (18.11)$$

The quantities in this expression (which is valid provided that ω is not close to ω_{n0}) are the same as those in the previous *Justification*, with $\hbar\omega_{n0} = E_n^{(0)} - E_0^{(0)}$. As $\omega \rightarrow 0$, the equation reduces to eqn 18.10 for the static polarizability. As ω becomes very high (and much higher than any excitation frequency of the molecule so that the ω_{n0}^2 in the denominator can be ignored), the polarizability becomes

$$\alpha(\omega) = -\frac{2}{\hbar\omega^2} \sum_n \omega_{n0} |\mu_{0n}|^2 \rightarrow 0 \quad \text{as} \quad \omega \rightarrow \infty$$

That is, when the incident frequency is much higher than any excitation frequency, the polarizability becomes zero. The argument applies to each type of excitation, vibrational as well as electronic, and accounts for the successive decreases in polarizability as the frequency is increased.

18.3 Relative permittivities

When two charges q_1 and q_2 are separated by a distance r in a vacuum, the potential energy of their interaction is (see Appendix 3):

$$V = \frac{q_1 q_2}{4\pi\epsilon_0 r} \quad (18.12a)$$

When the same two charges are immersed in a medium (such as air or a liquid), their potential energy is reduced to

$$V = \frac{q_1 q_2}{4\pi\epsilon r} \quad (18.12b)$$

where ϵ is the **permittivity** of the medium. The permittivity is normally expressed in terms of the dimensionless **relative permittivity**, ϵ_r , (formerly and still widely called the dielectric constant) of the medium:

$$\epsilon_r = \frac{\epsilon}{\epsilon_0} \quad [18.13]$$

The relative permittivity can have a very significant effect on the strength of the interactions between ions in solution. For instance, water has a relative permittivity of 78 at 25°C, so the interionic Coulombic interaction energy is reduced by nearly two orders of magnitude from its vacuum value. Some of the consequences of this reduction for electrolyte solutions were explored in Chapter 5.

The relative permittivity of a substance is large if its molecules are polar or highly polarizable. The quantitative relation between the relative permittivity and the electric properties of the molecules is obtained by considering the polarization of a medium, and is expressed by the **Debye equation** (for the derivation of this and the following equations, see *Further reading*):

$$\frac{\epsilon_r - 1}{\epsilon_r + 2} = \frac{\rho P_m}{M} \quad (18.14)$$

where ρ is the mass density of the sample, M is the molar mass of the molecules, and P_m is the **molar polarization**, which is defined as

$$P_m = \frac{N_A}{3\epsilon_0} \left(\alpha + \frac{\mu^2}{3kT} \right) \quad [18.15]$$

The term $\mu^2/3kT$ stems from the thermal averaging of the electric dipole moment in the presence of the applied field (eqn 18.5). The corresponding expression without the contribution from the permanent dipole moment is called the **Clausius–Mossotti equation**:

$$\frac{\epsilon_r - 1}{\epsilon_r + 2} = \frac{\rho N_A \alpha}{3M\epsilon_0} \quad (18.16)$$

The Clausius–Mossotti equation is used when there is no contribution from permanent electric dipole moments to the polarization, either because the molecules are non-polar or because the frequency of the applied field is so high that the molecules cannot orientate quickly enough to follow the change in direction of the field.

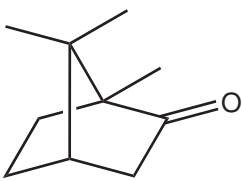
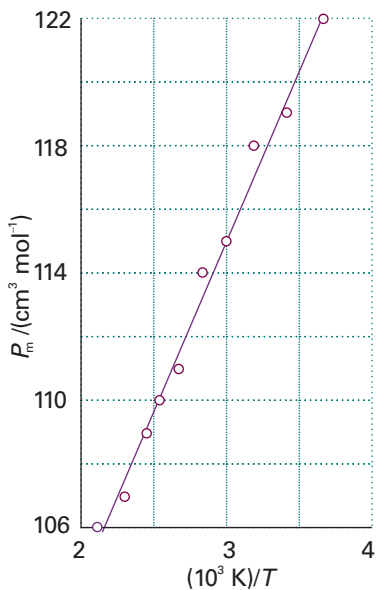
**8 Camphor**

Fig. 18.2 The plot of $P_m / (\text{cm}^3 \text{ mol}^{-1})$ against $(10^3 \text{ K})/T$ used in Example 18.2 for the determination of the polarizability and dipole moment of camphor.

Example 18.2 Determining dipole moment and polarizability

The relative permittivity of a substance is measured by comparing the capacitance of a capacitor with and without the sample present (C and C_0 , respectively) and using $\epsilon_r = C/C_0$. The relative permittivity of camphor (8) was measured at a series of temperatures with the results given below. Determine the dipole moment and the polarizability volume of the molecule.

| $\theta/^\circ\text{C}$ | $\rho / (\text{g cm}^{-3})$ | ϵ_r |
|-------------------------|-----------------------------|--------------|
| 0 | 0.99 | 12.5 |
| 20 | 0.99 | 11.4 |
| 40 | 0.99 | 10.8 |
| 60 | 0.99 | 10.0 |
| 80 | 0.99 | 9.50 |
| 100 | 0.99 | 8.90 |
| 120 | 0.97 | 8.10 |
| 140 | 0.96 | 7.60 |
| 160 | 0.95 | 7.11 |
| 200 | 0.91 | 6.21 |

Method Equation 18.14 implies that the polarizability and permanent electric dipole moment of the molecules in a sample can be determined by measuring ϵ_r at a series of temperatures, calculating P_m , and plotting it against $1/T$. The slope of the graph is $N_A \mu^2 / 9\epsilon_0 k$ and its intercept at $1/T = 0$ is $N_A \alpha / 3\epsilon_0$. We need to calculate $(\epsilon_r - 1)/(\epsilon_r + 2)$ at each temperature, and then multiply by M/ρ to form P_m .

Answer For camphor, $M = 152.23 \text{ g mol}^{-1}$. We can therefore use the data to draw up the following table:

| $\theta/^\circ\text{C}$ | $(10^3 \text{ K})/T$ | ϵ_r | $(\epsilon_r - 1)/(\epsilon_r + 2)$ | $P_m / (\text{cm}^3 \text{ mol}^{-1})$ |
|-------------------------|----------------------|--------------|-------------------------------------|--|
| 0 | 3.66 | 12.5 | 0.793 | 122 |
| 20 | 3.41 | 11.4 | 0.776 | 119 |
| 40 | 3.19 | 10.8 | 0.766 | 118 |
| 60 | 3.00 | 10.0 | 0.750 | 115 |
| 80 | 2.83 | 9.50 | 0.739 | 114 |
| 100 | 2.68 | 8.90 | 0.725 | 111 |
| 120 | 2.54 | 8.10 | 0.703 | 110 |
| 140 | 2.42 | 7.60 | 0.688 | 109 |
| 160 | 2.31 | 7.11 | 0.670 | 107 |
| 200 | 2.11 | 6.21 | 0.634 | 106 |

The points are plotted in Fig. 18.2. The intercept lies at 82.7, so $\alpha' = 3.3 \times 10^{-23} \text{ cm}^3$. The slope is 10.9, so $\mu = 4.46 \times 10^{-30} \text{ C m}$, corresponding to 1.34 D. Because the Debye equation describes molecules that are free to rotate, the data show that camphor, which does not melt until 175°C, is rotating even in the solid. It is an approximately spherical molecule.

Self-test 18.3 The relative permittivity of chlorobenzene is 5.71 at 20°C and 5.62 at 25°C. Assuming a constant density (1.11 g cm^{-3}), estimate its polarizability volume and dipole moment. [$1.4 \times 10^{-23} \text{ cm}^3$, 1.2 D]

The Maxwell equations that describe the properties of electromagnetic radiation (see *Further reading*) relate the refractive index at a (visible or ultraviolet) specified wavelength to the relative permittivity at that frequency:

$$n_r = \epsilon_r^{1/2} \quad (18.17)$$

Therefore, the molar polarization, P_m , and the molecular polarizability, α , can be measured at frequencies typical of visible light (about 10^{15} to 10^{16} Hz) by measuring the refractive index of the sample and using the Clausius–Mossotti equation.

Comment 18.6

The refractive index, n_r , of the medium is the ratio of the speed of light in a vacuum, c , to its speed c' in the medium: $n_r = c/c'$. A beam of light changes direction ('bends') when it passes from a region of one refractive index to a region with a different refractive index. See Appendix 3 for details.

Interactions between molecules

A **van der Waals interaction** is the attractive interaction between closed-shell molecules that depends on the distance between the molecules as $1/r^6$. In addition, there are interactions between ions and the partial charges of polar molecules and repulsive interactions that prevent the complete collapse of matter to nuclear densities. The repulsive interactions arise from Coulombic repulsions and, indirectly, from the Pauli principle and the exclusion of electrons from regions of space where the orbitals of neighbouring species overlap.

18.4 Interactions between dipoles

Most of the discussion in this section is based on the Coulombic potential energy of interaction between two charges (eqn 18.12a). We can easily adapt this expression to find the potential energy of a point charge and a dipole and to extend it to the interaction between two dipoles.

(a) The potential energy of interaction

We show in the *Justification* below that the potential energy of interaction between a point dipole $\mu_1 = q_1 l$ and the point charge q_2 in the arrangement shown in (9) is

$$V = -\frac{\mu_1 q_2}{4\pi\epsilon_0 r^2} \quad (18.18)$$

With μ in coulomb metres, q_2 in coulombs, and r in metres, V is obtained in joules. A **point dipole** is a dipole in which the separation between the charges is much smaller than the distance at which the dipole is being observed, $l \ll r$. The potential energy rises towards zero (the value at infinite separation of the charge and the dipole) more rapidly (as $1/r^2$) than that between two point charges (which varies as $1/r$) because, from the viewpoint of the point charge, the partial charges of the dipole seem to merge and cancel as the distance r increases (Fig. 18.3).

Justification 18.4 The interaction between a point charge and a point dipole

The sum of the potential energies of repulsion between like charges and attraction between opposite charges in the orientation shown in (9) is

$$V = \frac{1}{4\pi\epsilon_0} \left(-\frac{q_1 q_2}{r - \frac{1}{2}l} + \frac{q_1 q_2}{r + \frac{1}{2}l} \right) = \frac{q_1 q_2}{4\pi\epsilon_0 r} \left(-\frac{1}{1-x} + \frac{1}{1+x} \right)$$

where $x = l/2r$. Because $l \ll r$ for a point dipole, this expression can be simplified by expanding the terms in x and retaining only the leading term:

$$V = \frac{q_1 q_2}{4\pi\epsilon_0 r} \{ -(1+x+\dots) + (1-x+\dots) \} \approx -\frac{2x q_1 q_2}{4\pi\epsilon_0 r} = -\frac{q_1 q_2 l}{4\pi\epsilon_0 r^2}$$

With $\mu_1 = q_1 l$, this expression becomes eqn 18.18. This expression should be multiplied by $\cos \theta$ when the point charge lies at an angle θ to the axis of the dipole.

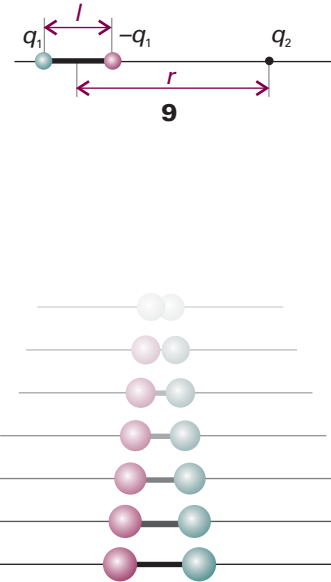


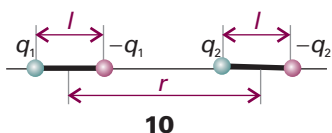
Fig. 18.3 There are two contributions to the diminishing field of an electric dipole with distance (here seen from the side). The potentials of the charges decrease (shown here by a fading intensity) and the two charges appear to merge, so their combined effect approaches zero more rapidly than by the distance effect alone.

Comment 18.7

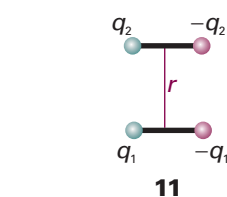
The following expansions are often useful:

$$\frac{1}{1+x} = 1 - x + x^2 - \dots$$

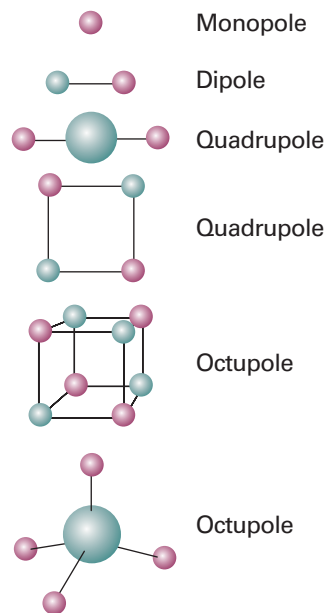
$$\frac{1}{1-x} = 1 + x + x^2 + \dots$$



10



11



Monopole

Dipole

Quadrupole

Quadrupole

Octupole

Octupole

Fig. 18.4 Typical charge arrays corresponding to electric multipoles. The field arising from an arbitrary finite charge distribution can be expressed as the superposition of the fields arising from a superposition of multipoles.

Example 18.3 Calculating the interaction energy of two dipoles

Calculate the potential energy of interaction of two dipoles in the arrangement shown in (10) when their separation is r .

Method We proceed in exactly the same way as in *Justification 18.4*, but now the total interaction energy is the sum of four pairwise terms, two attractions between opposite charges, which contribute negative terms to the potential energy, and two repulsions between like charges, which contribute positive terms.

Answer The sum of the four contributions is

$$V = \frac{1}{4\pi\epsilon_0} \left(-\frac{q_1 q_2}{r+l} + \frac{q_1 q_2}{r} + \frac{q_1 q_2}{r} - \frac{q_1 q_2}{r-l} \right) = -\frac{q_1 q_2}{4\pi\epsilon_0 r} \left(\frac{1}{1+x} - 2 + \frac{1}{1-x} \right)$$

with $x = l/r$. As before, provided $l \ll r$ we can expand the two terms in x and retain only the first surviving term, which is equal to $2x^2$. This step results in the expression

$$V = -\frac{2x q_1 q_2}{4\pi\epsilon_0 r}$$

Therefore, because $\mu_1 = q_1 l$ and $\mu_2 = q_2 l$, the potential energy of interaction in the alignment shown in the illustration is

$$V = -\frac{\mu_1 \mu_2}{2\pi\epsilon_0 r^3}$$

This interaction energy approaches zero more rapidly (as $1/r^3$) than for the previous case: now both interacting entities appear neutral to each other at large separations. See *Further information 18.1* for the general expression.

Self-test 18.4 Derive an expression for the potential energy when the dipoles are in the arrangement shown in (11). $[V = \mu_1 \mu_2 / 4\pi\epsilon_0 r^3]$

Table 18.3 summarizes the various expressions for the interaction of charges and dipoles. It is quite easy to extend the formulas given there to obtain expressions for the energy of interaction of higher **multipoles**, or arrays of point charges (Fig. 18.4). Specifically, an **n -pole** is an array of point charges with an n -pole moment but no lower moment. Thus, a **monopole** ($n = 1$) is a point charge, and the monopole moment is what we normally call the overall charge. A dipole ($n = 2$), as we have seen, is an array

Table 18.3 Multipole interaction potential energies

| Interaction type | Distance dependence of potential energy | Typical energy/ (kJ mol ⁻¹) | Comment |
|---------------------|---|--|------------------------------------|
| Ion-ion | $1/r$ | 250 | Only between ions* |
| Ion-dipole | $1/r^2$ | 15 | |
| Dipole-dipole | $1/r^3$ | 2 | Between stationary polar molecules |
| | $1/r^6$ | 0.6 | Between rotating polar molecules |
| London (dispersion) | $1/r^6$ | 2 | Between all types of molecules |

The energy of a hydrogen bond A—H···B is typically 20 kJ mol⁻¹ and occurs on contact for A, B = O, N, or F.

* Electrolyte solutions are treated in Chapter 5, ionic solids in Chapter 20.

of charges that has no monopole moment (no net charge). A **quadrupole** ($n = 3$) consists of an array of point charges that has neither net charge nor dipole moment (as for CO_2 molecules, 3). An **octupole** ($n = 4$) consists of an array of point charges that sum to zero and which has neither a dipole moment nor a quadrupole moment (as for CH_4 molecules, 12). The feature to remember is that the interaction energy falls off more rapidly the higher the order of the multipole. For the interaction of an n -pole with an m -pole, the potential energy varies with distance as

$$V \propto \frac{1}{r^{n+m-1}} \quad (18.19)$$

The reason for the even steeper decrease with distance is the same as before: the array of charges appears to blend together into neutrality more rapidly with distance the higher the number of individual charges that contribute to the multipole. Note that a given molecule may have a charge distribution that corresponds to a superposition of several different multipoles.

(b) The electric field

The same kind of argument as that used to derive expressions for the potential energy can be used to establish the distance dependence of the strength of the electric field generated by a dipole. We shall need this expression when we calculate the dipole moment induced in one molecule by another.

The starting point for the calculation is the strength of the electric field generated by a point electric charge:

$$E = \frac{q}{4\pi\epsilon_0 r^2} \quad (18.20)$$

The field generated by a dipole is the sum of the fields generated by each partial charge. For the point-dipole arrangement shown in Fig. 18.5, the same procedure that was used to derive the potential energy gives

$$E = \frac{\mu}{2\pi\epsilon_0 r^3} \quad (18.21)$$

The electric field of a multipole (in this case a dipole) decreases more rapidly with distance (as $1/r^3$ for a dipole) than a monopole (a point charge).

(c) Dipole-dipole interactions

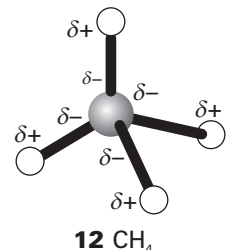
The potential energy of interaction between two polar molecules is a complicated function of their relative orientation. When the two dipoles are parallel (as in 13), the potential energy is simply (see *Further information 18.1*)

$$V = \frac{\mu_1 \mu_2 f(\theta)}{4\pi\epsilon_0 r^3} \quad f(\theta) = 1 - 3 \cos^2 \theta \quad (18.22)$$

This expression applies to polar molecules in a fixed, parallel, orientation in a solid.

In a fluid of freely rotating molecules, the interaction between dipoles averages to zero because $f(\theta)$ changes sign as the orientation changes, and its average value is zero. Physically, the like partial charges of two freely rotating molecules are close together as much as the two opposite charges, and the repulsion of the former is cancelled by the attraction of the latter.

The interaction energy of two *freely* rotating dipoles is zero. However, because their mutual potential energy depends on their relative orientation, the molecules do not in fact rotate completely freely, even in a gas. In fact, the lower energy orientations are



Comment 18.8

The electric field is actually a vector, and we cannot simply add and subtract magnitudes without taking into account the directions of the fields. In the cases we consider, this will not be a complication because the two charges of the dipoles will be collinear and give rise to fields in the same direction. Be careful, though, with more general arrangements of charges.

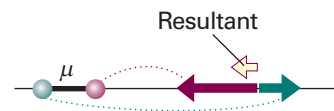
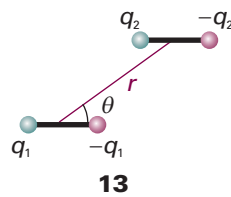


Fig. 18.5 The electric field of a dipole is the sum of the opposing fields from the positive and negative charges, each of which is proportional to $1/r^2$. The difference, the net field, is proportional to $1/r^3$.



Comment 18.9

The average (or mean value) of a function $f(x)$ over the range from $x = a$ to $x = b$ is

$$\langle f \rangle = \frac{1}{b-a} \int_a^b f(x) dx$$

The volume element in polar coordinates is proportional to $\sin \theta d\theta$, and θ ranges from 0 to π . Therefore the average value of $(1 - 3 \cos^2 \theta)$ is

$$(1/\pi) \int_0^\pi (1 - 3 \cos^2 \theta) \sin \theta d\theta = 0.$$

marginally favoured, so there is a nonzero average interaction between polar molecules. We show in the following *Justification* that the average potential energy of two rotating molecules that are separated by a distance r is

$$\langle V \rangle = -\frac{C}{r^6} \quad C = \frac{2\mu_1^2\mu_2^2}{3(4\pi\epsilon_0)^2 kT} \quad (18.23)$$

This expression describes the **Keesom interaction**, and is the first of the contributions to the van der Waals interaction.

Justification 18.5 The Keesom interaction

The detailed calculation of the Keesom interaction energy is quite complicated, but the form of the final answer can be constructed quite simply. First, we note that the average interaction energy of two polar molecules rotating at a fixed separation r is given by

$$\langle V \rangle = \frac{\mu_1\mu_2\langle f \rangle}{4\pi\epsilon_0 r^3}$$

where $\langle f \rangle$ now includes a weighting factor in the averaging that is equal to the probability that a particular orientation will be adopted. This probability is given by the Boltzmann distribution $p \propto e^{-E/kT}$, with E interpreted as the potential energy of interaction of the two dipoles in that orientation. That is,

$$p \propto e^{-V/kT} \quad V = \frac{\mu_1\mu_2 f}{4\pi\epsilon_0 r^3}$$

When the potential energy of interaction of the two dipoles is very small compared with the energy of thermal motion, we can use $V \ll kT$, expand the exponential function in p , and retain only the first two terms:

$$p \propto 1 - V/kT + \dots$$

The weighted average of f is therefore

$$\langle f \rangle = \langle f \rangle_0 - \frac{\mu_1\mu_2}{4\pi\epsilon_0 k T r^3} \langle f^2 \rangle_0 + \dots$$

where $\langle \dots \rangle_0$ denotes an unweighted spherical average. The spherical average of f is zero, so the first term vanishes. However, the average value of f^2 is nonzero because f^2 is positive at all orientations, so we can write

$$\langle V \rangle = -\frac{\mu_1^2\mu_2^2\langle f^2 \rangle_0}{(4\pi\epsilon_0)^2 k T r^6}$$

The average value $\langle f^2 \rangle_0$ turns out to be $\frac{2}{3}$ when the calculation is carried through in detail. The final result is that quoted in eqn 18.23.

The important features of eqn 18.23 are its negative sign (the average interaction is attractive), the dependence of the average interaction energy on the inverse sixth power of the separation (which identifies it as a van der Waals interaction), and its inverse dependence on the temperature. The last feature reflects the way that the greater thermal motion overcomes the mutual orientating effects of the dipoles at higher temperatures. The inverse sixth power arises from the inverse third power of the interaction potential energy that is weighted by the energy in the Boltzmann term, which is also proportional to the inverse third power of the separation.

At 25°C the average interaction energy for pairs of molecules with $\mu = 1$ D is about -0.07 kJ mol⁻¹ when the separation is 0.5 nm. This energy should be compared with

the average molar kinetic energy of $\frac{3}{2}RT = 3.7 \text{ kJ mol}^{-1}$ at the same temperature. The interaction energy is also much smaller than the energies involved in the making and breaking of chemical bonds.

(d) Dipole-induced-dipole interactions

A polar molecule with dipole moment μ_1 can induce a dipole μ_2^* in a neighbouring polarizable molecule (Fig. 18.6). The induced dipole interacts with the permanent dipole of the first molecule, and the two are attracted together. The average interaction energy when the separation of the molecules is r is (for a derivation, see *Further reading*)

$$V = -\frac{C}{r^6} \quad C = \frac{\mu_1^2 \alpha'_2}{4\pi\epsilon_0} \quad (18.24)$$

where α'_2 is the polarizability volume of molecule 2 and μ_1 is the permanent dipole moment of molecule 1. Note that the C in this expression is different from the C in eqn 18.23 and other expressions below: we are using the same symbol in C/r^6 to emphasize the similarity of form of each expression.

The dipole–induced-dipole interaction energy is independent of the temperature because thermal motion has no effect on the averaging process. Moreover, like the dipole–dipole interaction, the potential energy depends on $1/r^6$: this distance dependence stems from the $1/r^3$ dependence of the field (and hence the magnitude of the induced dipole) and the $1/r^3$ dependence of the potential energy of interaction between the permanent and induced dipoles. For a molecule with $\mu = 1 \text{ D}$ (such as HCl) near a molecule of polarizability volume $\alpha' = 10 \times 10^{-30} \text{ m}^3$ (such as benzene, Table 18.1), the average interaction energy is about -0.8 kJ mol^{-1} when the separation is 0.3 nm.

(e) Induced-dipole–induced-dipole interactions

Nonpolar molecules (including closed-shell atoms, such as Ar) attract one another even though neither has a permanent dipole moment. The abundant evidence for the existence of interactions between them is the formation of condensed phases of nonpolar substances, such as the condensation of hydrogen or argon to a liquid at low temperatures and the fact that benzene is a liquid at normal temperatures.

The interaction between nonpolar molecules arises from the transient dipoles that all molecules possess as a result of fluctuations in the instantaneous positions of electrons. To appreciate the origin of the interaction, suppose that the electrons in one molecule flicker into an arrangement that gives the molecule an instantaneous dipole moment μ_1^* . This dipole generates an electric field that polarizes the other molecule, and induces in that molecule an instantaneous dipole moment μ_2^* . The two dipoles attract each other and the potential energy of the pair is lowered. Although the first molecule will go on to change the size and direction of its instantaneous dipole, the electron distribution of the second molecule will follow; that is, the two dipoles are correlated in direction (Fig. 18.7). Because of this correlation, the attraction between the two instantaneous dipoles does not average to zero, and gives rise to an induced-dipole–induced-dipole interaction. This interaction is called either the **dispersion interaction** or the **London interaction** (for Fritz London, who first described it).

Polar molecules also interact by a dispersion interaction: such molecules also possess instantaneous dipoles, the only difference being that the time average of each fluctuating dipole does not vanish, but corresponds to the permanent dipole. Such molecules therefore interact both through their permanent dipoles and through the correlated, instantaneous fluctuations in these dipoles.

The strength of the dispersion interaction depends on the polarizability of the first molecule because the instantaneous dipole moment μ_1^* depends on the looseness of

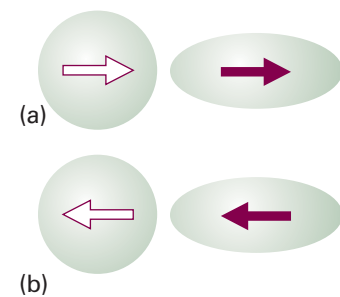


Fig. 18.6 (a) A polar molecule (purple arrow) can induce a dipole (white arrow) in a nonpolar molecule, and (b) the latter's orientation follows the former's, so the interaction does not average to zero.

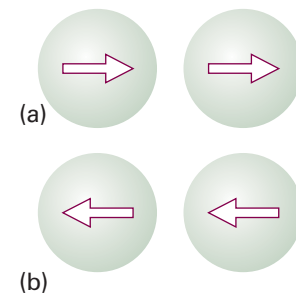


Fig. 18.7 (a) In the dispersion interaction, an instantaneous dipole on one molecule induces a dipole on another molecule, and the two dipoles then interact to lower the energy. (b) The two instantaneous dipoles are correlated and, although they occur in different orientations at different instants, the interaction does not average to zero.

the control that the nuclear charge exercises over the outer electrons. The strength of the interaction also depends on the polarizability of the second molecule, for that polarizability determines how readily a dipole can be induced by another molecule. The actual calculation of the dispersion interaction is quite involved, but a reasonable approximation to the interaction energy is given by the **London formula**:

$$V = -\frac{C}{r^6} \quad C = \frac{3}{2} \alpha'_1 \alpha'_2 \frac{I_1 I_2}{I_1 + I_2} \quad (18.25)$$

where I_1 and I_2 are the ionization energies of the two molecules (Table 10.4). This interaction energy is also proportional to the inverse sixth power of the separation of the molecules, which identifies it as a third contribution to the van der Waals interaction. The dispersion interaction generally dominates all the interactions between molecules other than hydrogen bonds.

Illustration 18.1 Calculating the strength of the dispersion interaction

For two CH_4 molecules, we can substitute $\alpha' = 2.6 \times 10^{-30} \text{ m}^3$ and $I \approx 700 \text{ kJ mol}^{-1}$ to obtain $V = -2 \text{ kJ mol}^{-1}$ for $r = 0.3 \text{ nm}$. A very rough check on this figure is the enthalpy of vaporization of methane, which is 8.2 kJ mol^{-1} . However, this comparison is insecure, partly because the enthalpy of vaporization is a many-body quantity and partly because the long-distance assumption breaks down.

(f) Hydrogen bonding

The interactions described so far are universal in the sense that they are possessed by all molecules independent of their specific identity. However, there is a type of interaction possessed by molecules that have a particular constitution. A **hydrogen bond** is an attractive interaction between two species that arises from a link of the form $\text{A}-\text{H} \cdots \text{B}$, where A and B are highly electronegative elements and B possesses a lone pair of electrons. Hydrogen bonding is conventionally regarded as being limited to N, O, and F but, if B is an anionic species (such as Cl^-), it may also participate in hydrogen bonding. There is no strict cutoff for an ability to participate in hydrogen bonding, but N, O, and F participate most effectively.

The formation of a hydrogen bond can be regarded either as the approach between a partial positive charge of H and a partial negative charge of B or as a particular example of delocalized molecular orbital formation in which A, H, and B each supply one atomic orbital from which three molecular orbitals are constructed (Fig. 18.8). Thus, if the $\text{A}-\text{H}$ bond is regarded as formed from the overlap of an orbital on A, ψ_A , and a hydrogen 1s orbital, ψ_H , and the lone pair on B occupies an orbital on B, ψ_B , then, when the two molecules are close together, we can build three molecular orbitals from the three basis orbitals:

$$\psi = c_1 \psi_A + c_2 \psi_H + c_3 \psi_B$$

One of the molecular orbitals is bonding, one almost nonbonding, and the third antibonding. These three orbitals need to accommodate four electrons (two from the original $\text{A}-\text{H}$ bond and two from the lone pair of B), so two enter the bonding orbital and two enter the nonbonding orbital. Because the antibonding orbital remains empty, the net effect—depending on the precise location of the almost nonbonding orbital—may be a lowering of energy.

In practice, the strength of the bond is found to be about 20 kJ mol^{-1} . Because the bonding depends on orbital overlap, it is virtually a contact-like interaction that is

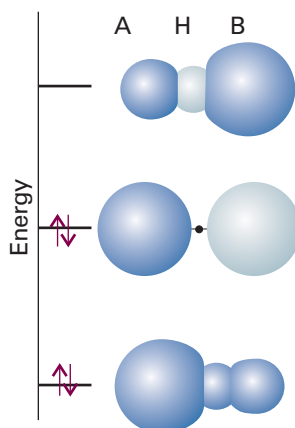


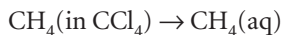
Fig. 18.8 The molecular orbital interpretation of the formation of an $\text{A}-\text{H} \cdots \text{B}$ hydrogen bond. From the three A, H, and B orbitals, three molecular orbitals can be formed (their relative contributions are represented by the sizes of the spheres). Only the two lower energy orbitals are occupied, and there may therefore be a net lowering of energy compared with the separate AH and B species.

turned on when AH touches B and is zero as soon as the contact is broken. If hydrogen bonding is present, it dominates the other intermolecular interactions. The properties of liquid and solid water, for example, are dominated by the hydrogen bonding between H₂O molecules. The structure of DNA and hence the transmission of genetic information is crucially dependent on the strength of hydrogen bonds between base pairs. The structural evidence for hydrogen bonding comes from noting that the internuclear distance between formally non-bonded atoms is less than their van der Waals contact distance, which suggests that a dominating attractive interaction is present. For example, the O—O distance in O—H…O is expected to be 280 pm on the basis of van der Waals radii, but is found to be 270 pm in typical compounds. Moreover, the H…O distance is expected to be 260 pm but is found to be only 170 pm.

Hydrogen bonds may be either symmetric or unsymmetric. In a symmetric hydrogen bond, the H atoms lies midway between the two other atoms. This arrangement is rare, but occurs in F—H…F⁻, where both bond lengths are 120 pm. More common is the unsymmetrical arrangement, where the A—H bond is shorter than the H…B bond. Simple electrostatic arguments, treating A—H…B as an array of point charges (partial negative charges on A and B, partial positive on H) suggest that the lowest energy is achieved when the bond is linear, because then the two partial negative charges are furthest apart. The experimental evidence from structural studies support a linear or near-linear arrangement.

(g) The hydrophobic interaction

Nonpolar molecules do dissolve slightly in polar solvents, but strong interactions between solute and solvent are not possible and as a result it is found that each individual solute molecule is surrounded by a solvent cage (Fig. 18.9). To understand the consequences of this effect, consider the thermodynamics of transfer of a nonpolar hydrocarbon solute from a nonpolar solvent to water, a polar solvent. Experiments indicate that the process is endergonic ($\Delta_{\text{transfer}}G > 0$), as expected on the basis of the increase in polarity of the solvent, but exothermic ($\Delta_{\text{transfer}}H < 0$). Therefore, it is a large decrease in the entropy of the system ($\Delta_{\text{transfer}}S < 0$) that accounts for the positive Gibbs energy of transfer. For example, the process



has $\Delta_{\text{transfer}}G = +12 \text{ kJ mol}^{-1}$, $\Delta_{\text{transfer}}H = -10 \text{ kJ mol}^{-1}$, and $\Delta_{\text{transfer}}S = -75 \text{ J K}^{-1} \text{ mol}^{-1}$ at 298 K. Substances characterized by a positive Gibbs energy of transfer from a nonpolar to a polar solvent are called **hydrophobic**.

It is possible to quantify the hydrophobicity of a small molecular group R by defining the **hydrophobicity constant**, π , as

$$\pi = \log \frac{S}{S_0} \quad [18.26]$$

where S is the ratio of the molar solubility of the compound R—A in octanol, a nonpolar solvent, to that in water, and S_0 is the ratio of the molar solubility of the compound H—A in octanol to that in water. Therefore, positive values of π indicate hydrophobicity and negative values of π indicate hydrophilicity, the thermodynamic preference for water as a solvent. It is observed experimentally that the π values of most groups do not depend on the nature of A. However, measurements do suggest group additivity of π values. For example, π for R = CH₃, CH₂CH₃, (CH₂)₂CH₃, (CH₂)₃CH₃, and (CH₂)₄CH₃ is, respectively, 0.5, 1.0, 1.5, 2.0, and 2.5 and we conclude that acyclic saturated hydrocarbons become more hydrophobic as the carbon chain length increases. This trend can be rationalized by $\Delta_{\text{transfer}}H$ becoming more positive and $\Delta_{\text{transfer}}S$ more negative as the number of carbon atoms in the chain increases.

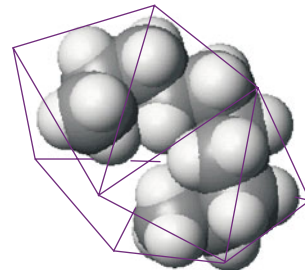


Fig. 18.9 When a hydrocarbon molecule is surrounded by water, the H₂O molecules form a clathrate cage. As a result of this acquisition of structure, the entropy of the water decreases, so the dispersal of the hydrocarbon into the water is entropy-opposed; its coalescence is entropy-favoured.

At the molecular level, formation of a solvent cage around a hydrophobic molecule involves the formation of new hydrogen bonds among solvent molecules. This is an exothermic process and accounts for the negative values of $\Delta_{\text{transfer}} H$. On the other hand, the increase in order associated with formation of a very large number of small solvent cages decreases the entropy of the system and accounts for the negative values of $\Delta_{\text{transfer}} S$. However, when many solute molecules cluster together, fewer (albeit larger) cages are required and more solvent molecules are free to move. The net effect of formation of large clusters of hydrophobic molecules is then a decrease in the organization of the solvent and therefore a net *increase* in entropy of the system. This increase in entropy of the solvent is large enough to render spontaneous the association of hydrophobic molecules in a polar solvent.

The increase in entropy that results from fewer structural demands on the solvent placed by the clustering of nonpolar molecules is the origin of the **hydrophobic interaction**, which tends to stabilize groupings of hydrophobic groups in micelles and biopolymers (Chapter 19). The hydrophobic interaction is an example of an ordering process that is stabilized by a tendency toward greater disorder of the solvent.

(h) The total attractive interaction

We shall consider molecules that are unable to participate in hydrogen bond formation. The total attractive interaction energy between rotating molecules is then the sum of the three van der Waals contributions discussed above. (Only the dispersion interaction contributes if both molecules are nonpolar.) In a fluid phase, all three contributions to the potential energy vary as the inverse sixth power of the separation of the molecules, so we may write

$$V = -\frac{C_6}{r^6} \quad (18.27)$$

where C_6 is a coefficient that depends on the identity of the molecules.

Although attractive interactions between molecules are often expressed as in eqn 18.27, we must remember that this equation has only limited validity. First, we have taken into account only dipolar interactions of various kinds, for they have the longest range and are dominant if the average separation of the molecules is large. However, in a complete treatment we should also consider quadrupolar and higher-order multipole interactions, particularly if the molecules do not have permanent electric dipole moments. Secondly, the expressions have been derived by assuming that the molecules can rotate reasonably freely. That is not the case in most solids, and in rigid media the dipole–dipole interaction is proportional to $1/r^3$ because the Boltzmann averaging procedure is irrelevant when the molecules are trapped into a fixed orientation.

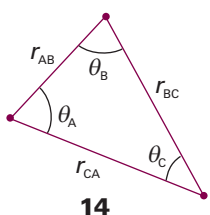
A different kind of limitation is that eqn 18.27 relates to the interactions of pairs of molecules. There is no reason to suppose that the energy of interaction of three (or more) molecules is the sum of the pairwise interaction energies alone. The total dispersion energy of three closed-shell atoms, for instance, is given approximately by the **Axilrod–Teller formula**:

$$V = -\frac{C_6}{r_{AB}^6} - \frac{C_6}{r_{BC}^6} - \frac{C_6}{r_{CA}^6} + \frac{C'}{(r_{AB} r_{BC} r_{CA})^3} \quad (18.28a)$$

where

$$C' = a(3 \cos \theta_A \cos \theta_B \cos \theta_C + 1) \quad (18.28b)$$

The parameter a is approximately equal to $\frac{3}{4}\alpha' C_6$; the angles θ are the internal angles of the triangle formed by the three atoms (14). The term in C' (which represents the non-additivity of the pairwise interactions) is negative for a linear arrangement of



atoms (so that arrangement is stabilized) and positive for an equilateral triangular cluster. It is found that the three-body term contributes about 10 per cent of the total interaction energy in liquid argon.

18.5 Repulsive and total interactions

When molecules are squeezed together, the nuclear and electronic repulsions and the rising electronic kinetic energy begin to dominate the attractive forces. The repulsions increase steeply with decreasing separation in a way that can be deduced only by very extensive, complicated molecular structure calculations of the kind described in Chapter 11 (Fig. 18.10).

In many cases, however, progress can be made by using a greatly simplified representation of the potential energy, where the details are ignored and the general features expressed by a few adjustable parameters. One such approximation is the **hard-sphere potential**, in which it is assumed that the potential energy rises abruptly to infinity as soon as the particles come within a separation d :

$$V = \infty \quad \text{for } r \leq d \quad V = 0 \quad \text{for } r > d \quad (18.29)$$

This very simple potential is surprisingly useful for assessing a number of properties. Another widely used approximation is the **Mie potential**:

$$V = \frac{C_n}{r^n} - \frac{C_m}{r^m} \quad (18.30)$$

with $n > m$. The first term represents repulsions and the second term attractions. The **Lennard-Jones potential** is a special case of the Mie potential with $n = 12$ and $m = 6$ (Fig. 18.11); it is often written in the form

$$V = 4\epsilon \left\{ \left(\frac{r_0}{r} \right)^{12} - \left(\frac{r_0}{r} \right)^6 \right\} \quad (18.31)$$

The two parameters are ϵ , the depth of the well (not to be confused with the symbol of the permittivity of a medium used in Section 18.3), and r_0 , the separation at which $V = 0$ (Table 18.4). The well minimum occurs at $r_e = 2^{1/6}r_0$. Although the Lennard-Jones potential has been used in many calculations, there is plenty of evidence to show that $1/r^{12}$ is a very poor representation of the repulsive potential, and that an exponential form, e^{-r/r_0} , is greatly superior. An exponential function is more faithful to the exponential decay of atomic wavefunctions at large distances, and hence to the overlap that is responsible for repulsion. The potential with an exponential repulsive term and a $1/r^6$ attractive term is known as an **exp-6 potential**. These potentials can be used to calculate the virial coefficients of gases, as explained in Section 17.5, and through them various properties of real gases, such as the Joule-Thompson coefficient. The potentials are also used to model the structures of condensed fluids.

With the advent of **atomic force microscopy** (AFM), in which the force between a molecular sized probe and a surface is monitored (see *Impact 19.1*), it has become possible to measure directly the forces acting between molecules. The force, F , is the negative slope of potential, so for a Lennard-Jones potential between individual molecules we write

$$F = -\frac{dV}{dr} = \frac{24\epsilon}{r_0} \left\{ 2 \left(\frac{r_0}{r} \right)^{13} - \left(\frac{r_0}{r} \right)^7 \right\} \quad (18.32)$$

The net attractive force is greatest (from $dF/dr = 0$) at $r = (\frac{26}{7})^{1/6}r_0$, or $1.244r_0$, and at that distance is equal to $-144(\frac{7}{26})^{7/6}\epsilon/13r_0$, or $-2.397\epsilon/r_0$. For typical parameters, the magnitude of this force is about 10 pN.

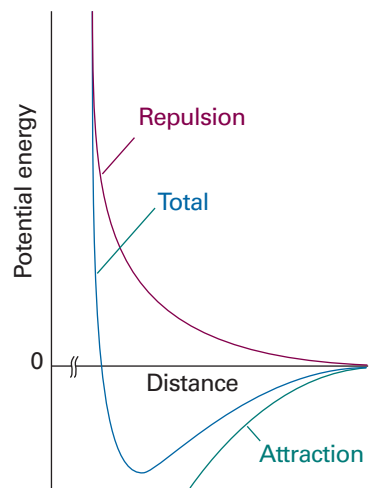


Fig. 18.10 The general form of an intermolecular potential energy curve. At long range the interaction is attractive, but at close range the repulsions dominate.

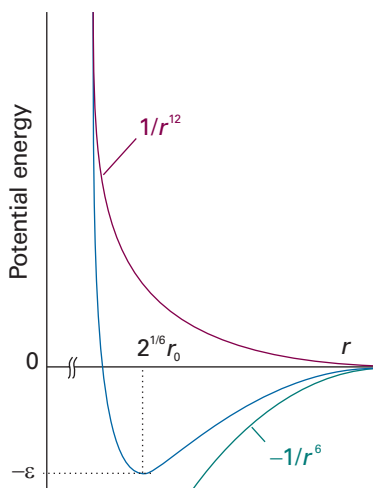


Fig. 18.11 The Lennard-Jones potential, and the relation of the parameters to the features of the curve. The green and purple lines are the two contributions.

Synoptic table 18.4* Lennard-Jones (12,6) parameters

| | (\epsilon/k)/K | r ₀ /pm |
|------------------|----------------|--------------------|
| Ar | 111.84 | 362.3 |
| CCl ₄ | 376.86 | 624.1 |
| N ₂ | 91.85 | 391.9 |
| Xe | 213.96 | 426.0 |

* More values are given in the *Data section*.

**IMPACT ON MEDICINE****I18.1 Molecular recognition and drug design**

A drug is a small molecule or protein that binds to a specific receptor site of a target molecule, such as a larger protein or nucleic acid, and inhibits the progress of disease. To devise efficient therapies, we need to know how to characterize and optimize molecular interactions between drug and target.

Molecular interactions are responsible for the assembly of many biological structures. Hydrogen bonding and hydrophobic interactions are primarily responsible for the three-dimensional structures of biopolymers, such as proteins, nucleic acids, and cell membranes. The binding of a ligand, or *guest*, to a biopolymer, or *host*, is also governed by molecular interactions. Examples of biological *host–guest complexes* include enzyme–substrate complexes, antigen–antibody complexes, and drug–receptor complexes. In all these cases, a site on the guest contains functional groups that can interact with complementary functional groups of the host. For example, a hydrogen bond donor group of the guest must be positioned near a hydrogen bond acceptor group of the host for tight binding to occur. It is generally true that many specific intermolecular contacts must be made in a biological host–guest complex and, as a result, a guest binds only hosts that are chemically similar. The strict rules governing molecular recognition of a guest by a host control every biological process, from metabolism to immunological response, and provide important clues for the design of effective drugs for the treatment of disease.

Interactions between nonpolar groups can be important in the binding of a guest to a host. For example, many enzyme active sites have hydrophobic pockets that bind nonpolar groups of a substrate. In addition to dispersion, repulsive, and hydrophobic interactions, π stacking interactions are also possible, in which the planar π systems of aromatic macrocycles lie one on top of the other, in a nearly parallel orientation. Such interactions are responsible for the stacking of hydrogen-bonded base pairs in DNA (Fig. 18.12). Some drugs with planar π systems, shown as a green rectangle in Fig. 18.12, are effective because they intercalate between base pairs through π stacking interactions, causing the helix to unwind slightly and altering the function of DNA.

Coulombic interactions can be important in the interior of a biopolymer host, where the relative permittivity can be much lower than that of the aqueous exterior. For example, at physiological pH, amino acid side chains containing carboxylic acid or amine groups are negatively and positively charged, respectively, and can attract each other. Dipole–dipole interactions are also possible because many of the building blocks of biopolymers are polar, including the peptide link, $-\text{CONH}-$ (see *Example 18.1*). However, hydrogen bonding interactions are by far the most prevalent in a biological host–guest complexes. Many effective drugs bind tightly and inhibit the action of enzymes that are associated with the progress of a disease. In many cases, a successful inhibitor will be able to form the same hydrogen bonds with the binding site that the normal substrate of the enzyme can form, except that the drug is chemically inert toward the enzyme.

There are two main strategies for the discovery of a drug. In *structure-based design*, new drugs are developed on the basis of the known structure of the receptor site of a known target. However, in many cases a number of so-called *lead compounds* are known to have some biological activity but little information is available about the target. To design a molecule with improved pharmacological efficacy, **quantitative structure–activity relationships** (QSAR) are often established by correlating data on activity of lead compounds with molecular properties, also called *molecular descriptors*, which can be determined either experimentally or computationally.

In broad terms, the first stage of the QSAR method consists of compiling molecular descriptors for a very large number of lead compounds. Descriptors such as molar

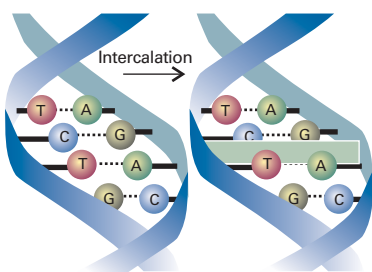


Fig. 18.12 Some drugs with planar π systems, shown as a green rectangle, intercalate between base pairs of DNA.

mass, molecular dimensions and volume, and relative solubility in water and nonpolar solvents are available from routine experimental procedures. Quantum mechanical descriptors determined by semi-empirical and *ab initio* calculations include bond orders and HOMO and LUMO energies.

In the second stage of the process, biological activity is expressed as a function of the molecular descriptors. An example of a QSAR equation is:

$$\text{Activity} = c_0 + c_1 d_1 + c_2 d_1^2 + c_3 d_2 + c_4 d_2^2 + \dots \quad (18.33)$$

where d_i is the value of the descriptor and c_i is a coefficient calculated by fitting the data by regression analysis. The quadratic terms account for the fact that biological activity can have a maximum or minimum value at a specific descriptor value. For example, a molecule might not cross a biological membrane and become available for binding to targets in the interior of the cell if it is too hydrophilic (water-loving), in which case it will not partition into the hydrophobic layer of the cell membrane (see Section 19.14 for details of membrane structure), or too hydrophobic (water-repelling), for then it may bind too tightly to the membrane. It follows that the activity will peak at some intermediate value of a parameter that measures the relative solubility of the drug in water and organic solvents.

In the final stage of the QSAR process, the activity of a drug candidate can be estimated from its molecular descriptors and the QSAR equation either by interpolation or extrapolation of the data. The predictions are more reliable when a large number of lead compounds and molecular descriptors are used to generate the QSAR equation.

The traditional QSAR technique has been refined into 3D QSAR, in which sophisticated computational methods are used to gain further insight into the three-dimensional features of drug candidates that lead to tight binding to the receptor site of a target. The process begins by using a computer to superimpose three-dimensional structural models of lead compounds and looking for common features, such as similarities in shape, location of functional groups, and electrostatic potential plots, which can be obtained from molecular orbital calculations. The key assumption of the method is that common structural features are indicative of molecular properties that enhance binding of the drug to the receptor. The collection of superimposed molecules is then placed inside a three-dimensional grid of points. An atomic probe, typically an sp^3 -hybridized carbon atom, visits each grid point and two energies of interaction are calculated: E_{steric} , the steric energy reflecting interactions between the probe and electrons in uncharged regions of the drug, and E_{elec} , the electrostatic energy arising from interactions between the probe and a region of the molecule carrying a partial charge. The measured equilibrium constant for binding of the drug to the target, K_{bind} , is then assumed to be related to the interaction energies at each point r by the 3D QSAR equation

$$\log K_{\text{bind}} = c_0 + \sum_r \{c_S(r)E_{\text{steric}}(r) + c_E(r)E_{\text{elec}}(r)\} \quad (18.34)$$

where the $c(r)$ are coefficients calculated by regression analysis, with the coefficients c_S and c_E reflecting the relative importance of steric and electrostatic interactions, respectively, at the grid point r . Visualization of the regression analysis is facilitated by colouring each grid point according to the magnitude of the coefficients. Figure 18.13 shows results of a 3D QSAR analysis of the binding of steroids, molecules with the carbon skeleton shown, to human corticosteroid-binding globulin (CBG). Indeed, we see that the technique lives up to the promise of opening a window into the chemical nature of the binding site even when its structure is not known.

The QSAR and 3D QSAR methods, though powerful, have limited power: the predictions are only as good as the data used in the correlations are both reliable and

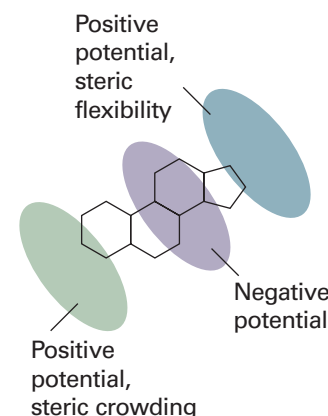


Fig. 18.13 A 3D QSAR analysis of the binding of steroids, molecules with the carbon skeleton shown, to human corticosteroid-binding globulin (CBG). The ellipses indicate areas in the protein's binding site with positive or negative electrostatic potentials and with little or much steric crowding. It follows from the calculations that addition of large substituents near the left-hand side of the molecule (as it is drawn on the page) leads to poor affinity of the drug to the binding site. Also, substituents that lead to the accumulation of negative electrostatic potential at either end of the drug are likely to show enhanced affinity for the binding site. (Adapted from P. Krogsgaard-Larsen, T. Liljefors, U. Madsen (ed.), *Textbook of drug design and discovery*, Taylor & Francis, London (2002).)

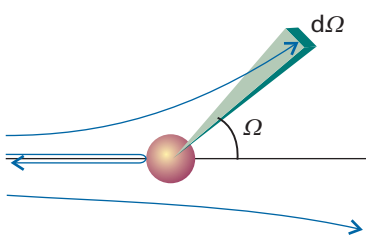


Fig. 18.14 The definition of the solid angle, $d\Omega$, for scattering.

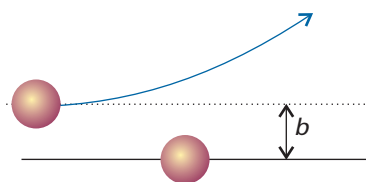


Fig. 18.15 The definition of the impact parameter, b , as the perpendicular separation of the initial paths of the particles.

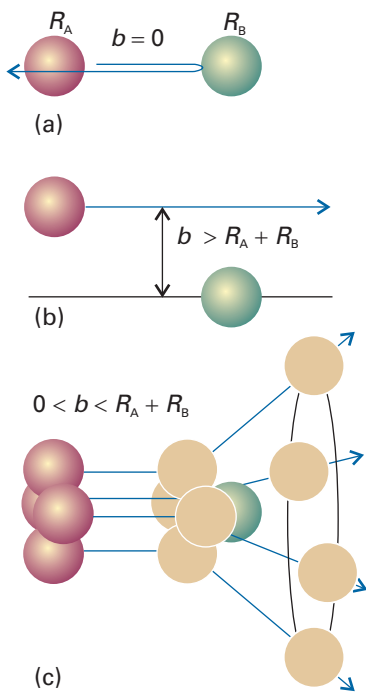


Fig. 18.16 Three typical cases for the collisions of two hard spheres: (a) $b = 0$, giving backward scattering; (b) $b > R_A + R_B$, giving forward scattering; (c) $0 < b < R_A + R_B$, leading to scattering into one direction on a ring of possibilities. (The target molecule is taken to be so heavy that it remains virtually stationary.)

abundant. However, the techniques have been used successfully to identify compounds that deserve further synthetic elaboration, such as addition or removal of functional groups, and testing.

Gases and liquids

The form of matter with the least order is a gas. In a perfect gas there are no intermolecular interactions and the distribution of molecules is completely random. In a real gas there are weak attractions and repulsions that have minimal effect on the relative locations of the molecules but that cause deviations from the perfect gas law for the dependence of pressure on the volume, temperature, and amount (Section 1.3).

The attractions between molecules are responsible for the condensation of gases into liquids at low temperatures. At low enough temperatures the molecules of a gas have insufficient kinetic energy to escape from each other's attraction and they stick together. Second, although molecules attract each other when they are a few diameters apart, as soon as they come into contact they repel each other. This repulsion is responsible for the fact that liquids and solids have a definite bulk and do not collapse to an infinitesimal point. The molecules are held together by molecular interactions, but their kinetic energies are comparable to their potential energies. As a result, we saw in Section 17.6 that, although the molecules of a liquid are not free to escape completely from the bulk, the whole structure is very mobile and we can speak only of the *average* relative locations of molecules. In the following sections we build on those concepts and add thermodynamic arguments to describe the surface of a liquid and the condensation of a gas into a liquid.

18.6 Molecular interactions in gases

Molecular interactions in the gas phase can be studied in **molecular beams**, which consist of a collimated, narrow stream of molecules travelling though an evacuated vessel. The beam is directed towards other molecules, and the scattering that occurs on impact is related to the intermolecular interactions.

The primary experimental information from a molecular beam experiment is the fraction of the molecules in the incident beam that are scattered into a particular direction. The fraction is normally expressed in terms of dI , the rate at which molecules are scattered into a cone that represents the area covered by the 'eye' of the detector (Fig. 18.14). This rate is reported as the **differential scattering cross-section**, σ , the constant of proportionality between the value of dI and the intensity, I , of the incident beam, the number density of target molecules, \mathcal{N} , and the infinitesimal path length dx through the sample:

$$dI = \sigma I \mathcal{N} dx \quad (18.35)$$

The value of σ (which has the dimensions of area) depends on the **impact parameter**, b , the initial perpendicular separation of the paths of the colliding molecules (Fig. 18.15), and the details of the intermolecular potential. The role of the impact parameter is most easily seen by considering the impact of two hard spheres (Fig. 18.16). If $b = 0$, the lighter projectile is on a trajectory that leads to a head-on collision, so the only scattering intensity is detected when the detector is at $\theta = \pi$. When the impact parameter is so great that the spheres do not make contact ($b > R_A + R_B$), there is no scattering and the scattering cross-section is zero at all angles except $\theta = 0$. Glancing blows, with $0 < b \leq R_A + R_B$, lead to scattering intensity in cones around the forward direction.

The scattering pattern of real molecules, which are not hard spheres, depends on the details of the intermolecular potential, including the anisotropy that is present when the molecules are non-spherical. The scattering also depends on the relative speed of approach of the two particles: a very fast particle might pass through the interaction region without much deflection, whereas a slower one on the same path might be temporarily captured and undergo considerable deflection (Fig. 18.17). The variation of the scattering cross-section with the relative speed of approach should therefore give information about the strength and range of the intermolecular potential.

A further point is that the outcome of collisions is determined by quantum, not classical, mechanics. The wave nature of the particles can be taken into account, at least to some extent, by drawing all classical trajectories that take the projectile particle from source to detector, and then considering the effects of interference between them.

Two quantum mechanical effects are of great importance. A particle with a certain impact parameter might approach the attractive region of the potential in such a way that the particle is deflected towards the repulsive core (Fig. 18.18), which then repels it out through the attractive region to continue its flight in the forward direction. Some molecules, however, also travel in the forward direction because they have impact parameters so large that they are undeflected. The wavefunctions of the particles that take the two types of path interfere, and the intensity in the forward direction is modified. The effect is called **quantum oscillation**. The same phenomenon accounts for the optical ‘glory effect’, in which a bright halo can sometimes be seen surrounding an illuminated object. (The coloured rings around the shadow of an aircraft cast on clouds by the Sun, and often seen in flight, is an example of an optical glory.)

The second quantum effect we need consider is the observation of a strongly enhanced scattering in a non-forward direction. This effect is called **rainbow scattering** because the same mechanism accounts for the appearance of an optical rainbow. The origin of the phenomenon is illustrated in Fig. 18.19. As the impact parameter decreases, there comes a stage at which the scattering angle passes through a maximum and the interference between the paths results in a strongly scattered beam. The **rainbow angle**, θ_r , is the angle for which $d\theta/db = 0$ and the scattering is strong.

Another phenomenon that can occur in certain beams is the capturing of one species by another. The vibrational temperature in supersonic beams is so low that **van der Waals molecules** may be formed, which are complexes of the form AB in which A and B are held together by van der Waals forces or hydrogen bonds. Large numbers of such molecules have been studied spectroscopically, including ArHCl, $(\text{HCl})_2$, ArCO₂, and (H₂O)₂. More recently, van der Waals clusters of water molecules have been pursued as far as (H₂O)₆. The study of their spectroscopic properties gives detailed information about the intermolecular potentials involved.

18.7 The liquid–vapour interface

So far, we have concentrated on the properties of gases. In Section 17.6, we described the structure of liquids. Now we turn our attention to the physical boundary between phases, such as the surface where solid is in contact with liquid or liquid is in contact with its vapour, has interesting properties. In this section we concentrate on the liquid–vapour interface, which is interesting because it is so mobile. Chapter 25 deals with solid surfaces and their important role in catalysis.

(a) Surface tension

Liquids tend to adopt shapes that minimize their surface area, for then the maximum number of molecules are in the bulk and hence surrounded by and interacting with neighbours. Droplets of liquids therefore tend to be spherical, because a sphere is the

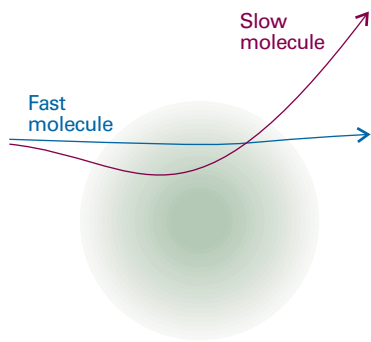


Fig. 18.17 The extent of scattering may depend on the relative speed of approach as well as the impact parameter. The darker central zone represents the repulsive core; the fuzzy outer zone represents the long-range attractive potential.

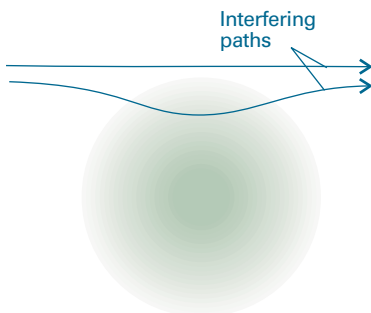


Fig. 18.18 Two paths leading to the same destination will interfere quantum mechanically; in this case they give rise to quantum oscillations in the forward direction.

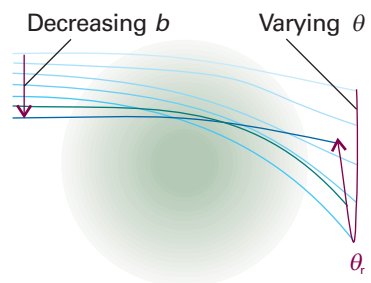


Fig. 18.19 The interference of paths leading to rainbow scattering. The rainbow angle, θ_r , is the maximum scattering angle reached as b is decreased. Interference between the numerous paths at that angle modifies the scattering intensity markedly.

Synoptic table 18.5* Surface tensions of liquids at 293 K

| | $\gamma /(\text{mN m}^{-1})^{\dagger}$ |
|----------|--|
| Benzene | 28.88 |
| Mercury | 472 |
| Methanol | 22.6 |
| Water | 72.75 |

* More values are given in the *Data section*.

[†] Note that $1 \text{ N m}^{-1} = 1 \text{ J m}^{-2}$.

shape with the smallest surface-to-volume ratio. However, there may be other forces present that compete against the tendency to form this ideal shape, and in particular gravity may flatten spheres into puddles or oceans.

Surface effects may be expressed in the language of Helmholtz and Gibbs energies (Chapter 3). The link between these quantities and the surface area is the work needed to change the area by a given amount, and the fact that dA and dG are equal (under different conditions) to the work done in changing the energy of a system. The work needed to change the surface area, σ , of a sample by an infinitesimal amount $d\sigma$ is proportional to $d\sigma$, and we write

$$dw = \gamma d\sigma \quad [18.36]$$

The constant of proportionality, γ , is called the **surface tension**; its dimensions are energy/area and its units are typically joules per metre squared (J m^{-2}). However, as in Table 18.5, values of γ are usually reported in newtons per metre (N m^{-1} , because $1 \text{ J} = 1 \text{ N m}$). The work of surface formation at constant volume and temperature can be identified with the change in the Helmholtz energy, and we can write

$$dA = \gamma d\sigma \quad (18.37)$$

Because the Helmholtz energy decreases ($dA < 0$) if the surface area decreases ($d\sigma < 0$), surfaces have a natural tendency to contract. This is a more formal way of expressing what we have already described.

Example 18.4 Using the surface tension

Calculate the work needed to raise a wire of length l and to stretch the surface of a liquid through a height h in the arrangement shown in Fig. 18.20. Disregard gravitational potential energy.

Method According to eqn 18.36, the work required to create a surface area given that the surface tension does not vary as the surface is formed is $w = \gamma\sigma$. Therefore, all we need do is to calculate the surface area of the two-sided rectangle formed as the frame is withdrawn from the liquid.

Answer When the wire of length l is raised through a height h it increases the area of the liquid by twice the area of the rectangle (because there is a surface on each side). The total increase is therefore $2lh$ and the work done is $2\gamma lh$. The work can be expressed as a force \times distance by writing it as $2\gamma l \times h$, and identifying γl as the opposing force on the wire of length l . This is why γ is called a tension and why its units are often chosen to be newtons per metre (N m^{-1} , so γl is a force in newtons).

Self-test 18.5 Calculate the work of creating a spherical cavity of radius r in a liquid of surface tension γ . $[4\pi r^2 \gamma]$

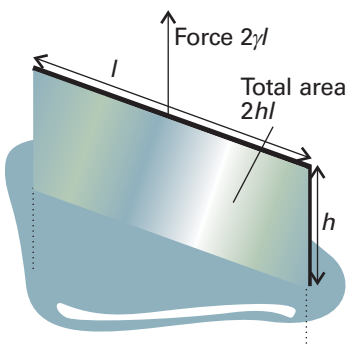


Fig. 18.20 The model used for calculating the work of forming a liquid film when a wire of length l is raised and pulls the surface with it through a height h .

(b) Curved surfaces

The minimization of the surface area of a liquid may result in the formation of a curved surface. A **bubble** is a region in which vapour (and possibly air too) is trapped by a thin film; a **cavity** is a vapour-filled hole in a liquid. What are widely called 'bubbles' in liquids are therefore strictly cavities. True bubbles have two surfaces (one on each side of the film); cavities have only one. The treatments of both are similar, but a factor of 2 is required for bubbles to take into account the doubled surface area. A **droplet** is a small volume of liquid at equilibrium surrounded by its vapour (and possibly also air).

The pressure on the concave side of an interface, p_{in} , is always greater than the pressure on the convex side, p_{out} . This relation is expressed by the **Laplace equation**, which is derived in the following *Justification*:

$$p_{\text{in}} = p_{\text{out}} + \frac{2\gamma}{r} \quad (18.38)$$

Justification 18.6 The Laplace equation

The cavities in a liquid are at equilibrium when the tendency for their surface area to decrease is balanced by the rise of internal pressure which would then result. When the pressure inside a cavity is p_{in} and its radius is r , the outward force is

$$\text{pressure} \times \text{area} = 4\pi r^2 p_{\text{in}}$$

The force inwards arises from the external pressure and the surface tension. The former has magnitude $4\pi r^2 p_{\text{out}}$. The latter is calculated as follows. The change in surface area when the radius of a sphere changes from r to $r + dr$ is

$$d\sigma = 4\pi(r + dr)^2 - 4\pi r^2 = 8\pi r dr$$

(The second-order infinitesimal, $(dr)^2$, is ignored.) The work done when the surface is stretched by this amount is therefore

$$dw = 8\pi\gamma r dr$$

As force \times distance is work, the force opposing stretching through a distance dr when the radius is r is

$$F = 8\pi\gamma r$$

The total inward force is therefore $4\pi r^2 p_{\text{out}} + 8\pi\gamma r$. At equilibrium, the outward and inward forces are balanced, so we can write

$$4\pi r^2 p_{\text{in}} = 4\pi r^2 p_{\text{out}} + 8\pi\gamma r$$

which rearranges into eqn 18.38.

The Laplace equation shows that the difference in pressure decreases to zero as the radius of curvature becomes infinite (when the surface is flat, Fig. 18.21). Small cavities have small radii of curvature, so the pressure difference across their surface is quite large. For instance, a ‘bubble’ (actually, a cavity) of radius 0.10 mm in champagne implies a pressure difference of 1.5 kPa, which is enough to sustain a column of water of height 15 cm.

(c) Capillary action

The tendency of liquids to rise up capillary tubes (tubes of narrow bore), which is called **capillary action**, is a consequence of surface tension. Consider what happens when a glass capillary tube is first immersed in water or any liquid that has a tendency to adhere to the walls. The energy is lowest when a thin film covers as much of the glass as possible. As this film creeps up the inside wall it has the effect of curving the surface of the liquid inside the tube. This curvature implies that the pressure just beneath the curving meniscus is less than the atmospheric pressure by approximately $2\gamma/r$, where r is the radius of the tube and we assume a hemispherical surface. The pressure immediately under the flat surface outside the tube is p , the atmospheric pressure; but inside the tube under the curved surface it is only $p - 2\gamma/r$. The excess external pressure presses the liquid up the tube until hydrostatic equilibrium (equal pressures at equal depths) has been reached (Fig. 18.22).

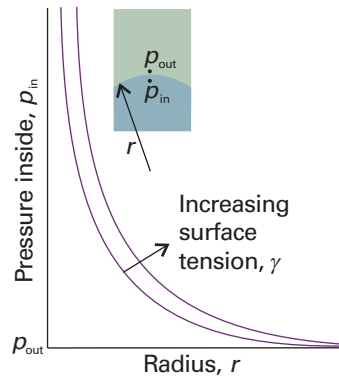


Fig. 18.21 The dependence of the pressure inside a curved surface on the radius of the surface, for two different values of the surface tension.

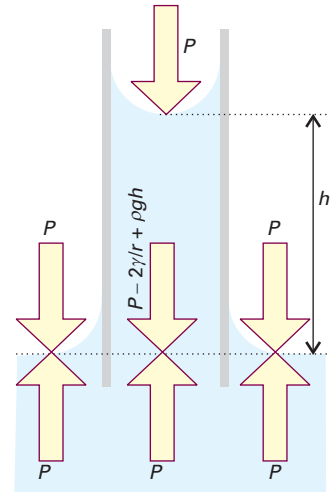


Fig. 18.22 When a capillary tube is first stood in a liquid, the latter climbs up the walls, so curving the surface. The pressure just under the meniscus is less than that arising from the atmosphere by $2\gamma/r$. The pressure is equal at equal heights throughout the liquid provided the hydrostatic pressure (which is equal to ρgh) cancels the pressure difference arising from the curvature.

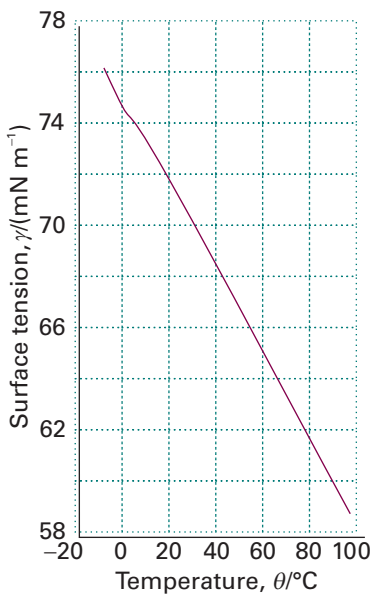


Fig. 18.23 The variation of the surface tension of water with temperature.

To calculate the height to which the liquid rises, we note that the pressure exerted by a column of liquid of mass density ρ and height h is

$$p = \rho gh \quad (18.39)$$

This hydrostatic pressure matches the pressure difference $2\gamma/r$ at equilibrium. Therefore, the height of the column at equilibrium is obtained by equating $2\gamma/r$ and ρgh , which gives

$$h = \frac{2\gamma}{\rho gr} \quad (18.40)$$

This simple expression provides a reasonably accurate way of measuring the surface tension of liquids. Surface tension decreases with increasing temperature (Fig. 18.23).

Illustration 18.2 Calculating the surface tension of a liquid from its capillary rise

If water at 25°C rises through 7.36 cm in a capillary of radius 0.20 mm, its surface tension at that temperature is

$$\begin{aligned} \gamma &= \frac{1}{2}\rho g h r \\ &= \frac{1}{2} \times (997.1 \text{ kg m}^{-3}) \times (9.81 \text{ m s}^{-2}) \times (7.36 \times 10^{-2} \text{ m}) \times (2.0 \times 10^{-4} \text{ m}) \\ &= 72 \text{ mN m}^{-1} \end{aligned}$$

where we have used $1 \text{ kg m s}^{-2} = 1 \text{ N}$.

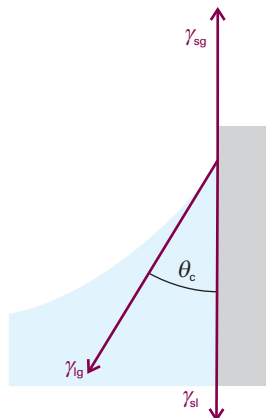


Fig. 18.24 The balance of forces that results in a contact angle, θ_c .

When the adhesive forces between the liquid and the material of the capillary wall are weaker than the cohesive forces within the liquid (as for mercury in glass), the liquid in the tube retracts from the walls. This retraction curves the surface with the concave, high pressure side downwards. To equalize the pressure at the same depth throughout the liquid the surface must fall to compensate for the heightened pressure arising from its curvature. This compensation results in a capillary depression.

In many cases there is a nonzero angle between the edge of the meniscus and the wall. If this contact angle is θ_c , then eqn 18.40 should be modified by multiplying the right-hand side by $\cos \theta_c$. The origin of the contact angle can be traced to the balance of forces at the line of contact between the liquid and the solid (Fig. 18.24). If the solid–gas, solid–liquid, and liquid–gas surface tensions (essentially the energy needed to create unit area of each of the interfaces) are denoted γ_{sg} , γ_{sl} , and γ_{lg} , respectively, then the vertical forces are in balance if

$$\gamma_{sg} = \gamma_{sl} + \gamma_{lg} \cos \theta_c \quad (18.41)$$

This expression solves to

$$\cos \theta_c = \frac{\gamma_{sg} - \gamma_{sl}}{\gamma_{lg}} \quad (18.42)$$

If we note that the superficial work of adhesion of the liquid to the solid (the work of adhesion divided by the area of contact) is

$$w_{ad} = \gamma_{sg} + \gamma_{lg} - \gamma_{sl} \quad (18.43)$$

eqn 18.42 can be written

$$\cos \theta_c = \frac{w_{ad}}{\gamma_{lg}} - 1 \quad (18.44)$$

We now see that the liquid ‘wets’ (spreads over) the surface, corresponding to $0 < \theta_c < 90^\circ$, when $1 < w_{ad}/\gamma_{lg} < 2$ (Fig. 18.25). The liquid does not wet the surface,

corresponding to $90^\circ < \theta_c < 180^\circ$, when $0 < w_{ad}/\gamma_{lg} < 1$. For mercury in contact with glass, $\theta_c = 140^\circ$, which corresponds to $w_{ad}/\gamma_{lg} = 0.23$, indicating a relatively low work of adhesion of the mercury to glass on account of the strong cohesive forces within mercury.

18.8 Condensation

We now bring together concepts from this chapter and Chapter 4 to explain the condensation of a gas to a liquid. We saw in Section 4.5 that the vapour pressure of a liquid depends on the pressure applied to the liquid. Because curving a surface gives rise to a pressure differential of $2\gamma/r$, we can expect the vapour pressure above a curved surface to be different from that above a flat surface. By substituting this value of the pressure difference into eqn 4.3 ($p = p^* e^{V_m \Delta P / RT}$, where p^* is the vapour pressure when the pressure difference is zero) we obtain the **Kelvin equation** for the vapour pressure of a liquid when it is dispersed as droplets of radius r :

$$p = p^* e^{2\gamma V_m / rRT} \quad (18.45)$$

The analogous expression for the vapour pressure inside a cavity can be written at once. The pressure of the liquid outside the cavity is less than the pressure inside, so the only change is in the sign of the exponent in the last expression.

For droplets of water of radius 1 μm and 1 nm the ratios p/p^* at 25°C are about 1.001 and 3, respectively. The second figure, although quite large, is unreliable because at that radius the droplet is less than about 10 molecules in diameter and the basis of the calculation is suspect. The first figure shows that the effect is usually small; nevertheless it may have important consequences.

Consider, for example, the formation of a cloud. Warm, moist air rises into the cooler regions higher in the atmosphere. At some altitude the temperature is so low that the vapour becomes thermodynamically unstable with respect to the liquid and we expect it to condense into a cloud of liquid droplets. The initial step can be imagined as a swarm of water molecules congregating into a microscopic droplet. Because the initial droplet is so small it has an enhanced vapour pressure. Therefore, instead of growing it evaporates. This effect stabilizes the vapour because an initial tendency to condense is overcome by a heightened tendency to evaporate. The vapour phase is then said to be **supersaturated**. It is thermodynamically unstable with respect to the liquid but not unstable with respect to the small droplets that need to form before the bulk liquid phase can appear, so the formation of the latter by a simple, direct mechanism is hindered.

Clouds do form, so there must be a mechanism. Two processes are responsible. The first is that a sufficiently large number of molecules might congregate into a droplet so big that the enhanced evaporative effect is unimportant. The chance of one of these **spontaneous nucleation centres** forming is low, and in rain formation it is not a dominant mechanism. The more important process depends on the presence of minute dust particles or other kinds of foreign matter. These **nucleate** the condensation (that is, provide centres at which it can occur) by providing surfaces to which the water molecules can attach.

Liquids may be **superheated** above their boiling temperatures and **supercooled** below their freezing temperatures. In each case the thermodynamically stable phase is not achieved on account of the kinetic stabilization that occurs in the absence of nucleation centres. For example, superheating occurs because the vapour pressure inside a cavity is artificially low, so any cavity that does form tends to collapse. This instability is encountered when an unstirred beaker of water is heated, for its temperature may be raised above its boiling point. Violent bumping often ensues as spontaneous nucleation leads to bubbles big enough to survive. To ensure smooth boiling at the true boiling temperature, nucleation centres, such as small pieces of sharp-edged glass or bubbles (cavities) of air, should be introduced.

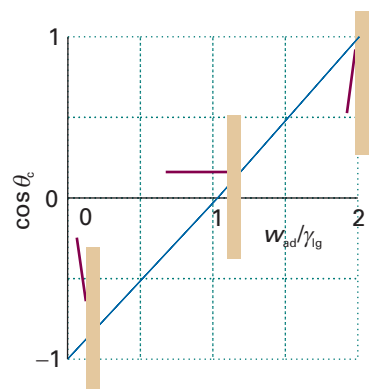


Fig. 18.25 The variation of contact angle (shown by the semaphore-like object) as the ratio w_{ad}/γ_{lg} changes.

Checklist of key ideas

- 1. A polar molecule is a molecule with a permanent electric dipole moment; the magnitude of a dipole moment is the product of the partial charge and the separation.
- 2. The polarization is the electric dipole moment density, $P = \langle \mu \rangle \mathcal{N}$. Orientation polarization is the polarization arising from the permanent dipole moments. Distortion polarization is the polarization arising from the distortion of the positions of the nuclei by the applied field.
- 3. The polarizability is a measure of the ability of an electric field to induce a dipole moment in a molecule ($\mu = \alpha E$). Electronic polarizability is the polarizability due to the distortion of the electron distribution.
- 4. The permittivity is the quantity ϵ in the Coulomb potential energy, $V = q_1 q_2 / 4\pi \epsilon r$.
- 5. The relative permittivity is given by $\epsilon_r = \epsilon / \epsilon_0$ and may be calculated from electric properties by using the Debye equation (eqn 18.14) or the Clausius–Mossotti equation (eqn 18.16).
- 6. A van der Waals interaction between closed-shell molecules is inversely proportional to the sixth power of their separation.
- 7. The potential energy of the dipole–dipole interaction between two fixed (non-rotating) molecules is proportional to $\mu_1 \mu_2 / r^3$ and that between molecules that are free to rotate is proportional to $\mu_1^2 \mu_2^2 / k T r^6$.
- 8. The dipole–induced-dipole interaction between two molecules is proportional to $\mu_1^2 \alpha_2 / r^6$, where α is the polarizability.
- 9. The potential energy of the dispersion (or London) interaction is proportional to $\alpha_1 \alpha_2 / r^6$.
- 10. A hydrogen bond is an interaction of the form A–H…B, where A and B are N, O, or F.
- 11. A hydrophobic interaction is an interaction that favours formation of clusters of hydrophobic groups in aqueous environments and that stems from changes in entropy of water molecules.
- 12. The Lennard-Jones (12,6) potential, $V = 4\epsilon \{(r_0/r)^{12} - (r_0/r)^6\}$, is a model of the total intermolecular potential energy.
- 13. A molecular beam is a collimated, narrow stream of molecules travelling through an evacuated vessel. Molecular beam techniques are used to investigate molecular interactions in gases.
- 14. The work of forming a liquid surface is $dW = \gamma d\sigma$, where γ is the surface tension.
- 15. The Laplace equation for the vapour pressure at a curved surface is $p_{in} = p_{out} + 2\gamma/r$.
- 16. The Kelvin equation for the vapour pressure of droplets is $p = p^* e^{2\gamma V_m / r k T}$.
- 17. Capillary action is the tendency of liquids to rise up capillary tubes.
- 18. Nucleation provides surfaces to which molecules can attach and thereby induce condensation.

Further reading

Articles and texts

- P.W. Atkins and R.S. Friedman, *Molecular quantum mechanics*. Oxford University Press (2005).
- M.A.D. Fluendy and K.P. Lawley, *Chemical applications of molecular beam scattering*. Chapman and Hall, London (1973).
- J.N. Israelachvili, *Intermolecular and surface forces*. Academic Press, New York (1998).
- G.A. Jeffrey, *An introduction to hydrogen bonding*. Oxford University Press (1997).

H.-J. Schneider and A. Yatsimirsky, *Principles and methods in supramolecular chemistry*. Wiley, Chichester (1999).

Sources of data and information

- J.J. Jasper, The surface tension of pure liquid compounds. *J. Phys. Chem. Ref. Data* **1**, 841 (1972).
- D.R. Lide (ed.), *CRC Handbook of Chemistry and Physics*, Sections 3, 4, 6, 9, 10, 12, and 13. CRC Press, Boca Raton (2000).

Further information

Further information 18.1 The dipole–dipole interaction

An important problem in physical chemistry is the calculation of the potential energy of interaction between two point dipoles with moments μ_1 and μ_2 , separated by a vector \mathbf{r} . From classical

electromagnetic theory, the potential energy of μ_2 in the electric field \mathbf{E}_1 generated by μ_1 is given by the dot (scalar) product

$$V = -\mathbf{E}_1 \cdot \mu_2 \quad (18.46)$$

To calculate \mathbf{E}_1 , we consider a distribution of point charges q_i located at x_i , y_i , and z_i from the origin. The Coulomb potential ϕ due to this distribution at a point with coordinates x , y , and z is:

$$\phi = \sum_i \frac{q_i}{4\pi\epsilon_0} \frac{1}{\{(x-x_i)^2 + (y-y_i)^2 + (z-z_i)^2\}^{1/2}} \quad (18.47)$$

Comment 18.10

The potential energy of a charge q_1 in the presence of another charge q_2 may be written as $V = q_1\phi$, where $\phi = q_2/4\pi\epsilon_0 r$ is the Coulomb potential. If there are several charges q_2, q_3, \dots present in the system, then the total potential experienced by the charge q_1 is the sum of the potential generated by each charge: $\phi = \phi_2 + \phi_3 + \dots$. The electric field strength is the negative gradient of the electric potential: $\mathbf{E} = -\nabla\phi$. See Appendix 3 for more details.

where r is the location of the point of interest and the r_i are the locations of the charges q_i . If we suppose that all the charges are close to the origin (in the sense that $r_i \ll r$), we can use a Taylor expansion to write

$$\begin{aligned} \phi(\mathbf{r}) &= \sum_i \frac{q_i}{4\pi\epsilon_0} \left\{ \frac{1}{r} + \left(\frac{\partial \{(x-x_i)^2 + (y-y_i)^2 + (z-z_i)^2\}^{1/2}}{\partial x_i} \right)_{x_i=0} x_i + \dots \right\} \\ &= \sum_i \frac{q_i}{4\pi\epsilon_0} \left\{ \frac{1}{r} + \frac{xx_i}{r^3} + \dots \right\} \end{aligned} \quad (18.48)$$

where the ellipses include the terms arising from derivatives with respect to y_i and z_i and higher derivatives. If the charge distribution is electrically neutral, the first term disappears because $\sum_i q_i = 0$. Next we note that $\sum_i q_i x_i = \mu_x$, and likewise for the y - and z -components. That is,

$$\phi = \frac{1}{4\pi\epsilon_0 r^3} (\mu_x x + \mu_y y + \mu_z z) = \frac{1}{4\pi\epsilon_0 r^3} \boldsymbol{\mu}_1 \cdot \mathbf{r} \quad (18.49)$$

The electric field strength is (see Comment 18.10)

$$\mathbf{E}_1 = \frac{1}{4\pi\epsilon_0} \nabla \frac{\boldsymbol{\mu}_1 \cdot \mathbf{r}}{r^3} = -\frac{\boldsymbol{\mu}_1}{4\pi\epsilon_0 r^3} - \frac{\boldsymbol{\mu}_1 \cdot \mathbf{r}}{4\pi\epsilon_0} \nabla \frac{1}{r^3} \quad (18.50)$$

It follows from eqns 18.46 and 18.50 that

$$V = \frac{\boldsymbol{\mu}_1 \cdot \boldsymbol{\mu}_2}{4\pi\epsilon_0 r^3} - 3 \frac{(\boldsymbol{\mu}_1 \cdot \mathbf{r})(\boldsymbol{\mu}_2 \cdot \mathbf{r})}{4\pi\epsilon_0 r^5} \quad (18.51)$$

For the arrangement shown in (13), in which $\boldsymbol{\mu}_1 \cdot \mathbf{r} = \mu_1 r \cos \theta$ and $\boldsymbol{\mu}_2 \cdot \mathbf{r} = \mu_2 r \cos \theta$, eqn 18.51 becomes:

$$V = \frac{\mu_1 \mu_2 f(\theta)}{4\pi\epsilon_0 r^3} \quad f(\theta) = 1 - 3 \cos^2 \theta \quad (18.52)$$

which is eqn 18.22.

Further information 18.2 The basic principles of molecular beams

The basic arrangement for a molecular beam experiment is shown in Fig. 18.26. If the pressure of vapour in the source is increased so that the mean free path of the molecules in the emerging beam is much shorter than the diameter of the pinhole, many collisions take place even outside the source. The net effect of these collisions, which give rise to **hydrodynamic flow**, is to transfer momentum into the

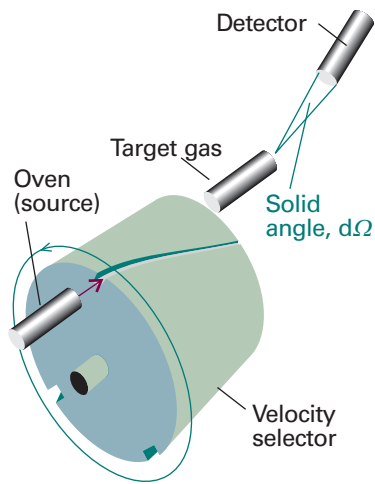


Fig. 18.26 The basic arrangement of a molecular beam apparatus. The atoms or molecules emerge from a heated source, and pass through the velocity selector, a rotating slotted cylinder such as that discussed in Section 1.3a. The scattering occurs from the target gas (which might take the form of another beam), and the flux of particles entering the detector set at some angle is recorded.

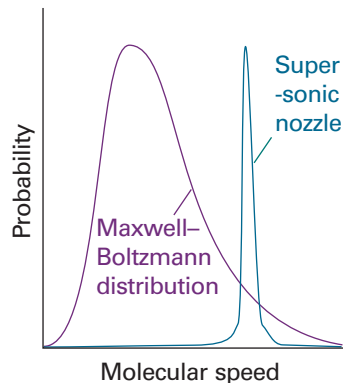


Fig. 18.27 The shift in the mean speed and the width of the distribution brought about by use of a supersonic nozzle.

direction of the beam. The molecules in the beam then travel with very similar speeds, so further downstream few collisions take place between them. This condition is called **molecular flow**. Because the spread in speeds is so small, the molecules are effectively in a state of very low translational temperature (Fig. 18.27). The translational temperature may reach as low as 1 K. Such jets are called **supersonic** because the average speed of the molecules in the jet is much greater than the speed of sound for the molecules that are not part of the jet.

A supersonic jet can be converted into a more parallel **supersonic beam** if it is 'skimmed' in the region of hydrodynamic flow and the excess gas pumped away. A skimmer consists of a conical nozzle shaped to avoid any supersonic shock waves spreading back into the gas and so increasing the translational temperature (Fig. 18.28). A jet or beam may also be formed by using helium or neon as the principal

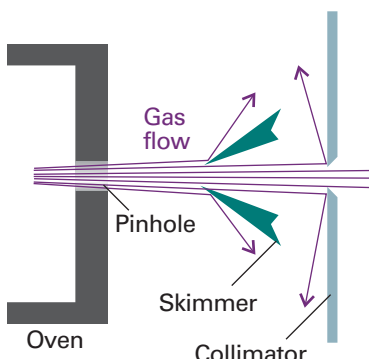


Fig. 18.28 A supersonic nozzle skims off some of the molecules of the beam and leads to a beam with well defined velocity.

gas, and injecting molecules of interest into it in the hydrodynamic region of flow.

The low translational temperature of the molecules is reflected in the low rotational and vibrational temperatures of the molecules. In

this context, a rotational or vibrational temperature means the temperature that should be used in the Boltzmann distribution to reproduce the observed populations of the states. However, as rotational modes equilibrate more slowly, and vibrational modes equilibrate even more slowly, the rotational and vibrational populations of the species correspond to somewhat higher temperatures, of the order of 10 K for rotation and 100 K for vibrations.

The target gas may be either a bulk sample or another molecular beam. The latter **crossed beam technique** gives a lot of information because the states of both the target and projectile molecules may be controlled. The intensity of the incident beam is measured by the **incident beam flux**, I , which is the number of particles passing through a given area in a given interval divided by the area and the duration of the interval.

The detectors may consist of a chamber fitted with a sensitive pressure gauge, a bolometer (a detector that responds to the incident energy by making use of the temperature-dependence of resistance), or an ionization detector, in which the incoming molecule is first ionized and then detected electronically. The state of the scattered molecules may also be determined spectroscopically, and is of interest when the collisions change their vibrational or rotational states.

Discussion questions

18.1 Explain how the permanent dipole moment and the polarizability of a molecule arise.

18.2 Explain why the polarizability of a molecule decreases at high frequencies.

18.3 Describe the experimental procedures available for determining the electric dipole moment of a molecule.

18.4 Account for the theoretical conclusion that many attractive interactions between molecules vary with their separation as $1/r^6$.

18.5 Describe the formation of a hydrogen bond in terms of molecular orbitals.

18.6 Account for the hydrophobic interaction and discuss its manifestations.

18.7 Describe how molecular beams are used to investigate intermolecular potentials.

Exercises

18.1a Which of the following molecules may be polar: ClF_3 , O_3 , H_2O_2 ?

18.1b Which of the following molecules may be polar: SO_3 , XeF_4 , SF_4 ?

18.2a The electric dipole moment of toluene (methylbenzene) is 0.4 D. Estimate the dipole moments of the three xylenes (dimethylbenzene). Which answer can you be sure about?

18.2b Calculate the resultant of two dipole moments of magnitude 1.5 D and 0.80 D that make an angle of 109.5° to each other.

18.3a Calculate the magnitude and direction of the dipole moment of the following arrangement of charges in the xy -plane: $3e$ at $(0, 0)$, $-e$ at $(0.32 \text{ nm}, 0)$, and $-2e$ at an angle of 20° from the x -axis and a distance of 0.23 nm from the origin.

18.3b Calculate the magnitude and direction of the dipole moment of the following arrangement of charges in the xy -plane: $4e$ at $(0, 0)$, $-2e$ at $(162 \text{ pm}, 0)$, and $-2e$ at an angle of 30° from the x -axis and a distance of 143 pm from the origin.

18.4a The molar polarization of fluorobenzene vapour varies linearly with T^{-1} , and is $70.62 \text{ cm}^3 \text{ mol}^{-1}$ at 351.0 K and $62.47 \text{ cm}^3 \text{ mol}^{-1}$ at 423.2 K . Calculate the polarizability and dipole moment of the molecule.

18.4b The molar polarization of the vapour of a compound was found to vary linearly with T^{-1} , and is $75.74 \text{ cm}^3 \text{ mol}^{-1}$ at 320.0 K and $71.43 \text{ cm}^3 \text{ mol}^{-1}$ at 421.7 K . Calculate the polarizability and dipole moment of the molecule.

18.5a At 0°C , the molar polarization of liquid chlorine trifluoride is $27.18 \text{ cm}^3 \text{ mol}^{-1}$ and its density is 1.89 g cm^{-3} . Calculate the relative permittivity of the liquid.

18.5b At 0°C , the molar polarization of a liquid is $32.16 \text{ cm}^3 \text{ mol}^{-1}$ and its density is 1.92 g cm^{-3} . Calculate the relative permittivity of the liquid. Take $M = 55.0 \text{ g mol}^{-1}$.

18.6a The polarizability volume of H_2O is $1.48 \times 10^{-24} \text{ cm}^3$; calculate the dipole moment of the molecule (in addition to the permanent dipole moment) induced by an applied electric field of strength 1.0 kV cm^{-1} .

18.6b The polarizability volume of NH_3 is $2.22 \times 10^{-30} \text{ m}^3$; calculate the dipole moment of the molecule (in addition to the permanent dipole moment) induced by an applied electric field of strength 15.0 kV m^{-1} .

18.7a The refractive index of CH_2I_2 is 1.732 for 656 nm light. Its density at 20°C is 3.32 g cm^{-3} . Calculate the polarizability of the molecule at this wavelength.

18.7b The refractive index of a compound is 1.622 for 643 nm light. Its density at 20°C is 2.99 g cm⁻³. Calculate the polarizability of the molecule at this wavelength. Take $M = 65.5 \text{ g mol}^{-1}$.

18.8a The polarizability volume of H₂O at optical frequencies is $1.5 \times 10^{-24} \text{ cm}^3$: estimate the refractive index of water. The experimental value is 1.33; what may be the origin of the discrepancy?

18.8b The polarizability volume of a liquid of molar mass 72.3 g mol⁻¹ and density 865 kg mol⁻¹ at optical frequencies is $2.2 \times 10^{-30} \text{ m}^3$: estimate the refractive index of the liquid.

18.9a The dipole moment of chlorobenzene is 1.57 D and its polarizability volume is $1.23 \times 10^{-23} \text{ cm}^3$. Estimate its relative permittivity at 25°C, when its density is 1.173 g cm⁻³.

18.9b The dipole moment of bromobenzene is $5.17 \times 10^{-30} \text{ C m}$ and its polarizability volume is approximately $1.5 \times 10^{-29} \text{ m}^3$. Estimate its relative permittivity at 25°C, when its density is 1491 kg m⁻³.

18.10a Calculate the vapour pressure of a spherical droplet of water of radius 10 nm at 20°C. The vapour pressure of bulk water at that temperature is 2.3 kPa and its density is 0.9982 g cm⁻³.

18.10b Calculate the vapour pressure of a spherical droplet of water of radius 20.0 nm at 35.0°C. The vapour pressure of bulk water at that temperature is 5.623 kPa and its density is 994.0 kg m⁻³.

18.11a The contact angle for water on clean glass is close to zero. Calculate the surface tension of water at 20°C given that at that temperature water climbs to a height of 4.96 cm in a clean glass capillary tube of internal radius 0.300 mm. The density of water at 20°C is 998.2 kg m⁻³.

18.11b The contact angle for water on clean glass is close to zero. Calculate the surface tension of water at 30°C given that at that temperature water climbs to a height of 9.11 cm in a clean glass capillary tube of internal radius 0.320 mm. The density of water at 30°C is 995.6 g cm⁻³.

18.12a Calculate the pressure differential of water across the surface of a spherical droplet of radius 200 nm at 20°C.

18.12b Calculate the pressure differential of ethanol across the surface of a spherical droplet of radius 220 nm at 20°C. The surface tension of ethanol at that temperature is 22.39 mN m⁻¹.

Problems*

Numerical problems

18.1 Suppose an H₂O molecule ($\mu = 1.85 \text{ D}$) approaches an anion. What is the favourable orientation of the molecule? Calculate the electric field (in volts per metre) experienced by the anion when the water dipole is (a) 1.0 nm, (b) 0.3 nm, (c) 30 nm from the ion.

18.2 An H₂O molecule is aligned by an external electric field of strength 1.0 kV m⁻¹ and an Ar atom ($\alpha' = 1.66 \times 10^{-24} \text{ cm}^3$) is brought up slowly from one side. At what separation is it energetically favourable for the H₂O molecule to flip over and point towards the approaching Ar atom?

18.3 The relative permittivity of chloroform was measured over a range of temperatures with the following results:

| $\theta/\text{^{\circ}C}$ | -80 | -70 | -60 | -40 | -20 | 0 | 20 |
|---------------------------|------|------|------|------|------|------|------|
| ϵ_r | 3.1 | 3.1 | 7.0 | 6.5 | 6.0 | 5.5 | 5.0 |
| $\rho/(\text{g cm}^{-3})$ | 1.65 | 1.64 | 1.64 | 1.61 | 1.57 | 1.53 | 1.50 |

The freezing point of chloroform is -64°C. Account for these results and calculate the dipole moment and polarizability volume of the molecule.

18.4 The relative permittivities of methanol (m.p. -95°C) corrected for density variation are given below. What molecular information can be deduced from these values? Take $\rho = 0.791 \text{ g cm}^{-3}$ at 20°C.

| $\theta/\text{^{\circ}C}$ | -185 | -170 | -150 | -140 | -110 | -80 | -50 | -20 | 0 | 20 |
|---------------------------|------|------|------|------|------|-----|-----|-----|----|----|
| ϵ_r | 3.2 | 3.6 | 4.0 | 5.1 | 67 | 57 | 4 | 43 | 38 | 34 |

18.5 In his classic book *Polar molecules*, Debye reports some early measurements of the polarizability of ammonia. From the selection below, determine the dipole moment and the polarizability volume of the molecule.

| T/K | 292.2 | 309.0 | 333.0 | 387.0 | 413.0 | 446.0 |
|--------------------------------------|-------|-------|-------|-------|-------|-------|
| $P_m/(\text{cm}^3 \text{ mol}^{-1})$ | 57.57 | 55.01 | 51.22 | 44.99 | 42.51 | 39.59 |

The refractive index of ammonia at 273 K and 100 kPa is 1.000 379 (for yellow sodium light). Calculate the molar polarizability of the gas at this temperature

and at 292.2 K. Combine the value calculated with the static molar polarizability at 292.2 K and deduce from this information alone the molecular dipole moment.

18.6 Values of the molar polarization of gaseous water at 100 kPa as determined from capacitance measurements are given below as a function of temperature.

| T/K | 384.3 | 420.1 | 444.7 | 484.1 | 522.0 |
|--------------------------------------|-------|-------|-------|-------|-------|
| $P_m/(\text{cm}^3 \text{ mol}^{-1})$ | 57.4 | 53.5 | 50.1 | 46.8 | 43.1 |

Calculate the dipole moment of H₂O and its polarizability volume.

18.7‡ F. Luo, G.C. McBane, O. Kim, C.F. Giese, and W.R. Gentry (*J. Chem. Phys.* **98**, 3564 (1993)) reported experimental observation of the He₂ complex, a species that had escaped detection for a long time. The fact that the observation required temperatures in the neighbourhood of 1 mK is consistent with computational studies which suggest that hcD_0 for He₂ is about $1.51 \times 10^{-23} \text{ J}$, hcD_0 about $2 \times 10^{-26} \text{ J}$, and R about 297 pm. (a) Determine the Lennard-Jones parameters r_0 and ϵ and plot the Lennard-Jones potential for He–He interactions. (b) Plot the Morse potential given that $a = 5.79 \times 10^{10} \text{ m}^{-1}$.

18.8‡ D.D. Nelson, G.T. Fraser, and W. Klemperer (*Science* **238**, 1670 (1987)) examined several weakly bound gas-phase complexes of ammonia in search of examples in which the H atoms in NH₃ formed hydrogen bonds, but found none. For example, they found that the complex of NH₃ and CO₂ has the carbon atom nearest the nitrogen (299 pm away): the CO₂ molecule is at right angles to the C–N ‘bond’, and the H atoms of NH₃ are pointing away from the CO₂. The permanent dipole moment of this complex is reported as 1.77 D. If the N and C atoms are the centres of the negative and positive charge distributions, respectively, what is the magnitude of those partial charges (as multiples of e)?

18.9‡ From data in Table 18.1 calculate the molar polarization, relative permittivity, and refractive index of methanol at 20°C. Its density at that temperature is 0.7914 g cm⁻³.

* Problems denoted with the symbol‡ were supplied by Charles Trapp and Carmen Giunta.

Theoretical problems

18.10 Calculate the potential energy of the interaction between two linear quadrupoles when they are (a) collinear, (b) parallel and separated by a distance r .

18.11 Show that, in a gas (for which the refractive index is close to 1), the refractive index depends on the pressure as $n_r = 1 + \text{const} \times p$, and find the constant of proportionality. Go on to show how to deduce the polarizability volume of a molecule from measurements of the refractive index of a gaseous sample.

18.12 Acetic acid vapour contains a proportion of planar, hydrogen-bonded dimers. The relative permittivity of pure liquid acetic acid is 7.14 at 290 K and increases with increasing temperature. Suggest an interpretation of the latter observation. What effect should isothermal dilution have on the relative permittivity of solutions of acetic acid in benzene?

18.13 Show that the mean interaction energy of N atoms of diameter d interacting with a potential energy of the form C_6/R^6 is given by $U = -2N^2C_6/3Vd^3$, where V is the volume in which the molecules are confined and all effects of clustering are ignored. Hence, find a connection between the van der Waals parameter a and C_6 , from $n^2aV^2 = (\partial U/\partial V)_T$.

18.14 Suppose the repulsive term in a Lennard-Jones (12,6)-potential is replaced by an exponential function of the form e^{-rd} . Sketch the form of the potential energy and locate the distance at which it is a minimum.

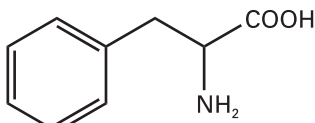
18.15 The *cohesive energy density*, \mathcal{V} , is defined as U/V , where U is the mean potential energy of attraction within the sample and V its volume. Show that $\mathcal{V} = \frac{1}{2}\mathcal{N}\int V(R)d\tau$, where \mathcal{N} is the number density of the molecules and $V(R)$ is their attractive potential energy and where the integration ranges from d to infinity and over all angles. Go on to show that the cohesive energy density of a uniform distribution of molecules that interact by a van der Waals attraction of the form $-C_6/R^6$ is equal to $(2\pi/3)(N_A^2/d^3M^2)\rho^2C_6$, where ρ is the mass density of the solid sample and M is the molar mass of the molecules.

18.16 Consider the collision between a hard-sphere molecule of radius R_1 and mass m , and an infinitely massive impenetrable sphere of radius R_2 . Plot the scattering angle θ as a function of the impact parameter b . Carry out the calculation using simple geometrical considerations.

18.17 The dependence of the scattering characteristics of atoms on the energy of the collision can be modelled as follows. We suppose that the two colliding atoms behave as impenetrable spheres, as in Problem 18.16, but that the effective radius of the heavy atoms depends on the speed v of the light atom. Suppose its effective radius depends on v as R_2e^{-v/v^*} , where v^* is a constant. Take $R_1 = \frac{1}{2}R_2$ for simplicity and an impact parameter $b = \frac{1}{2}R_2$, and plot the scattering angle as a function of (a) speed, (b) kinetic energy of approach.

Applications: to biochemistry

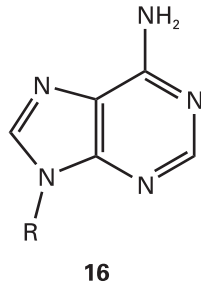
18.18 Phenylalanine (Phe, 15) is a naturally occurring amino acid. What is the energy of interaction between its phenyl group and the electric dipole moment of a neighbouring peptide group? Take the distance between the groups as 4.0 nm and treat the phenyl group as a benzene molecule. The dipole moment of the peptide group is $\mu = 2.7$ D and the polarizability volume of benzene is $\alpha' = 1.04 \times 10^{-29} \text{ m}^3$.



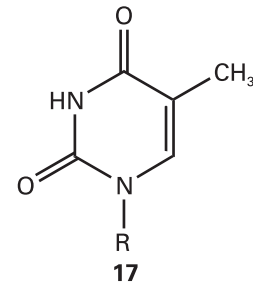
15

18.19 Now consider the London interaction between the phenyl groups of two Phe residues (see Problem 18.18). (a) Estimate the potential energy of interaction between two such rings (treated as benzene molecules) separated by 4.0 nm. For the ionization energy, use $I = 5.0$ eV. (b) Given that force is the negative slope of the potential, calculate the distance dependence of the force acting between two nonbonded groups of atoms, such as the phenyl groups of Phe, in a polypeptide chain that can have a London dispersion interaction with each other. What is the separation at which the force between the phenyl groups (treated as benzene molecules) of two Phe residues is zero? Hint. Calculate the slope by considering the potential energy at r and $r + \delta r$, with $\delta r \ll r$, and evaluating $\{V(r + \delta r) - V(r)\}/\delta r$. At the end of the calculation, let δr become vanishingly small.

18.20 Molecular orbital calculations may be used to predict structures of intermolecular complexes. Hydrogen bonds between purine and pyrimidine bases are responsible for the double helix structure of DNA (see Chapter 19). Consider methyl-adenine (16, with $R = \text{CH}_3$) and methyl-thymine (17, with $R = \text{CH}_3$) as models of two bases that can form hydrogen bonds in DNA. (a) Using molecular modelling software and the computational method of your choice, calculate the atomic charges of all atoms in methyl-adenine and methyl-thymine. (b) Based on your tabulation of atomic charges, identify the atoms in methyl-adenine and methyl-thymine that are likely to participate in hydrogen bonds. (c) Draw all possible adenine–thymine pairs that can be linked by hydrogen bonds, keeping in mind that linear arrangements of the A–H···B fragments are preferred in DNA. For this step, you may want to use your molecular modelling software to align the molecules properly. (d) Consult Chapter 19 and determine which of the pairs that you drew in part (c) occur naturally in DNA molecules. (e) Repeat parts (a)–(d) for cytosine and guanine, which also form base pairs in DNA (see Chapter 19 for the structures of these bases).

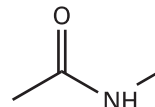


16



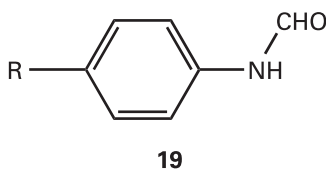
17

18.21 Molecular orbital calculations may be used to predict the dipole moments of molecules. (a) Using molecular modelling software and the computational method of your choice, calculate the dipole moment of the peptide link, modelled as a *trans*-*N*-methylacetamide (18). Plot the energy of interaction between these dipoles against the angle θ for $r = 3.0$ nm (see eqn 18.22). (b) Compare the maximum value of the dipole–dipole interaction energy from part (a) to 20 kJ mol⁻¹, a typical value for the energy of a hydrogen-bonding interaction in biological systems.



18

18.22 This problem gives a simple example of a quantitative structure–activity relation (QSAR). The binding of nonpolar groups of amino acid to hydrophobic sites in the interior of proteins is governed largely by hydrophobic interactions. (a) Consider a family of hydrocarbons R–H. The



hydrophobicity constants, π , for $R = \text{CH}_3, \text{CH}_2\text{CH}_3, (\text{CH}_2)_2\text{CH}_3, (\text{CH}_2)_3\text{CH}_3$, and $(\text{CH}_2)_4\text{CH}_3$ are, respectively, 0.5, 1.0, 1.5, 2.0, and 2.5. Use these data to predict the π value for $(\text{CH}_2)_6\text{CH}_3$. (b) The equilibrium constants K_I for the dissociation of inhibitors (**19**) from the enzyme chymotrypsin were measured for different substituents R:

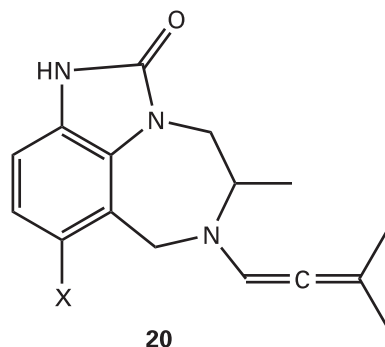
| R | CH_3CO | CN | NO_2 | CH_3 | Cl |
|------------|------------------------|--------|---------------|---------------|-------|
| π | -0.20 | -0.025 | 0.33 | 0.5 | 0.9 |
| $\log K_I$ | -1.73 | -1.90 | -2.43 | -2.55 | -3.40 |

Plot $\log K_I$ against π . Does the plot suggest a linear relationship? If so, what are the slope and intercept to the $\log K_I$ axis of the line that best fits the data? (c) Predict the value of K_I for the case $R = \text{H}$.

18.23 Derivatives of the compound TIBO (**20**) inhibit the enzyme reverse transcriptase, which catalyses the conversion of retroviral RNA to DNA. A QSAR analysis of the activity A of a number of TIBO derivatives suggests the following equation:

$$\log A = b_0 + b_1 S + b_2 W$$

where S is a parameter related to the drug's solubility in water and W is a parameter related to the width of the first atom in a substituent X shown in **20**.



(a) Use the following data to determine the values of b_0 , b_1 , and b_2 . Hint. The QSAR equation relates one dependent variable, $\log A$, to two independent variables, S and W . To fit the data, you must use the mathematical procedure of *multiple regression*, which can be performed with mathematical software or an electronic spreadsheet.

| X | H | Cl | SCH_3 | OCH_3 | CN | CHO | Br | CH_3 | CCH |
|-------|------|------|----------------|----------------|------|------|------|---------------|------|
| log A | 7.36 | 8.37 | 8.3 | 7.47 | 7.25 | 6.73 | 8.52 | 7.87 | 7.53 |
| S | 3.53 | 4.24 | 4.09 | 3.45 | 2.96 | 2.89 | 4.39 | 4.03 | 3.80 |
| W | 1.00 | 1.80 | 1.70 | 1.35 | 1.60 | 1.60 | 1.95 | 1.60 | 1.60 |

(b) What should be the value of W for a drug with $S = 4.84$ and $\log A = 7.60$?